

International Journal of Modern Physics D
 © World Scientific Publishing Company

NUMERICAL RELATIVITY FOR HORNDESKI GRAVITY

JUSTIN L. RIPLEY

*Department of Applied Mathematics and Theoretical Physics,
 University of Cambridge, Cambridge, CB3 0WA, United Kingdom*

*Illinois Center for Advanced Studies of the Universe & Department of Physics, University of
 Illinois at Urbana-Champaign, Urbana, Illinois 61801, USA*

ripley@illinois.edu

Received Day Month Year
 Revised Day Month Year

We present an overview of recent developments in the numerical solution of Horndeski gravity theories, which are the class of all scalar-tensor theories of gravity that have second order equations of motion. We review several methods that have been used to establish well-posed initial value problems for these theories, and discuss well-posed formulations of the constraint equations. We also discuss global aspects of exact, strongly coupled solutions to some of Horndeski gravity theories: the formation of shocks, the loss of hyperbolicity, and the formation of naked curvature singularities. Finally we discuss numerical solutions to binary black hole and neutron star systems for several Horndeski theories.

Keywords: Numerical relativity; Black holes; Modified gravity

PACS numbers:

Contents

1. Introduction	3
2. Horndeski gravity	5
3. Local well-posedness of the equations of motion	7
3.1. General considerations	7
3.2. Weakly-coupled regime	8
4. Local well-posedness of the <i>perturbative</i> equations of motion	9
5. Local well-posedness of the <i>exact</i> equations of motion	11
5.1. Well posed formulations of quadratic Horndeski gravity	11
5.2. Well-posed formulation of Cubic Horndeski gravity	12
5.3. Well-posed formulations of Bergmann–Wagoner scalar-tensor gravity theories	12
5.4. A well-posed formulation for all Horndeski gravity theories: the modified generalized harmonic (MGH) formulation	13

6. Exact solutions to the <i>fixed</i> equations of motion	15
7. Challenges to constructing global solutions to Horndeski theories	16
7.1. Local versus global solutions	16
7.2. Exact equations: failure of hyperbolicity in the strongly-coupled regime	19
7.3. Exact equations: shock/caustic formation	21
7.4. Perturbative solutions: secular instabilities, and the numerical dynamical renormalization group	22
8. Constructing exact initial data	23
8.1. The constraint equations: general properties	24
8.2. Example: the elliptic character of the exact constraint equations under the conformal transverse-traceless (CTT) decomposition	25
8.3. Example: Bowen-York “puncture” initial data in $4\partial ST$ gravity	28
9. Evolution of compact objects in Horndeski gravity theories: a brief survey of numerical work	30
9.1. Bergmann–Wagoner scalar-tensor theories	30
9.2. Quadratic Horndeski gravity	30
9.3. Cubic Horndeski gravity	31
9.4. $4\partial ST$ gravity (alias Einstein scalar Gauss–Bonnet (ESGB) gravity) .	32
10. Final remarks	33
Appendix A. Equations of motion for Horndeski gravity	33
Appendix B. Hyperbolicity and well-posedness of evolution (hyperbolic) partial differential equations	35
Appendix B.1. Well-posedness	36
Appendix B.2. Characteristics and notions of hyperbolicity	36
Appendix B.3. Physical interpretation of characteristics	38
Appendix C. Mixed-type partial differential equations	38
Appendix C.1. Two-dimensional PDE	38
Appendix C.2. Systems of PDE in higher dimensions	40
Appendix C.3. Example of a mixed-type PDE from Horndeski gravity .	40
Appendix D. General properties of the principal symbol for Horndeski gravity	42
Appendix D.1. Definitions	42
Appendix D.2. General symmetries of the principal symbol	43
Appendix D.3. The main theorem about the principal symbol	44
Appendix D.4. Physical characteristics and the lack of second time derivatives in the constraint equations	44
Appendix E. Identities for the $3 + 1$ decomposition of spacetime, and conformal transverse-traceless decomposition	45
Appendix F. $4\partial ST$ gravity as a gradient expansion about General Relativity with a scalar field	46

1. Introduction

Due to the complicated structure of the Einstein equations, understanding the merger of black holes and neutron stars—where gravity is in the *strong field, dynamical regime*—requires the use of computers to solve the equations of motion.^{1,2} A key technical step that led to the first stable numerical simulations of binary black hole systems in General Relativity (GR) was the construction of well-posed formulations of the Einstein equations.^{3–6} Since then, the observation of binary black holes (and neutron stars) by the LIGO/Virgo/KAGRA collaboration^{7–9} has spurred interest in understanding how modifications to GR could affect the classical dynamics of those objects.^{10–12} As of the writing of this review, the gravitational wave observations of binary black holes and neutron stars by the LIGO/Virgo/KAGRA collaboration have so far been found to be consistent with the predictions of GR.^{10,13–16} Despite this, as model-dependent tests of GR can allow for more precise tests of GR, there has been an extensive effort by many researchers to model the dynamics of binary black holes and neutron stars in *modified* (non-GR) theories of gravity.^{11,12}

The Horndeski theories,^{17–19} which encompass all theories of gravity that have a scalar and tensor field and that have second order equations of motion, have attracted particular attention as they allow for scalar “hairy” black hole and neutron star solutions,^{20–22} and have been used to model dark energy^{23a}. As was the case for GR around 25 years ago, a major challenge to numerically solving the equations of motion for Horndeski (and other modified) theories of gravity has been in constructing well-posed formulations of their equations of motion, that also allow for numerically stable evolution of black holes and neutron stars.^{25–31} An additional challenge to constructing numerical solutions in these theories has been in determining the properties of *global* solutions to Horndeski equations. Despite these challenges, recent mathematical and numerical relativity work indicates that it should be possible to simulate binary black hole/neutron star mergers for most, if not all, of the Horndeski gravity theories of astrophysical and cosmological interest.

In this review, we summarize recent work on the local and global properties of solutions to the Horndeski gravity theories, along with numerical relativity studies of the Horndeski gravity theories in the context of binary black hole/neutron star systems. Here we are purely concerned with the classical evolution of Horndeski gravity theories. We do not discuss the quantum mechanical viability of any particular Horndeski theory, although we note that as these theories have second order equations of motion, naive quantization of the theories do not suffer from the *Ostrogradski instability*.^{32,33} We do not provide a detailed review of the current observational and theoretical constraints on the Horndeski gravity theories, nor do we discuss other methods to construct solutions to the Horndeski gravity theories, such as Post-Newtonian methods. Finally, we do not discuss recent generalizations

^aWe note though that many Horndeski models that have been used to model energy are have been highly constrained by recent gravitational wave measurements; for one example constraint see 24

of the Horndeski gravity theories.³³

A brief summary of what we cover:

We first discuss a generic perturbative *order-reduction scheme*, which when applied to the Horndeski equations of motion, always leads to a strongly hyperbolic system of evolution equations and to elliptic constraint equations, with no restriction of the nature of the solutions (Sec. 4). The disadvantage of this approach is the *secular growth* of errors which generically occur in higher order perturbative solutions. These may be addressed via the *numerical dynamical renormalization group* (Sec. 7.4), although that technique has yet to be applied to the Horndeski gravity theories.

We next turn to *direct* approaches to solving the Horndeski equations of motion, that is approaches that solve the complete Horndeski equations of motion without approximation. Despite the considerable complexity of the Horndeski equations of motion (see Appendix A), their general structure as partial differential equations (PDE) are remarkably similar to the Einstein equations.^{30,31,34–36} For *weakly-coupled* solutions (Sec. 3.2), the equations of motion can be cast into a strongly hyperbolic form (Sec. 5), and the constraint equations can be recast as a set of elliptic partial differential equations (Sec. 8). For *strongly-coupled* solutions, some of the Horndeski theories can break down in a way not seen in solutions to the Einstein equations: shocks can form from smooth initial data^b, the equations of motion can lose their hyperbolic properties in *elliptic regions*, and curvature singularities may form (Sec. 7). Elliptic regions and curvature singularities can form *outside* of event horizons for some Horndeski theories. As both indicate a loss of predictivity, those theories have solutions that violate weak cosmic censorship^{38–41} (the formation of elliptic regions and/or curvature singularities could potentially be prevented by *fixing* the equations of motion, although more work remains to show this can always be done; see Sec. 6). This being said, the predominant view of Horndeski theories is that they should be viewed as parametrizing *effective* deviations from the Einstein equations. With this point of view, the breakdown of a Horndeski theory in a given solution can be interpreted as that solution lying outside the regime of applicability of the theory, and not that it is invalid to ever make use of that theory.

We present the full equations of motion for Horndeski gravity in Appendix A. We provide a short review of the basic concepts of well-posedness of evolution equations in Appendix B, and of mixed-type partial differential equation in Appendix C. We discuss some more general properties of the principal symbol of the Horndeski gravity theories in Appendix D, and collect a few identities that are useful for deriving the constraint equations of the Horndeski gravity theories in Appendix E. We review an effective field theory-styled “derivation” of Einstein scalar Gauss-Bonnet gravity (a Horndeski gravity theories that has attracted particular attention because it admits scalar hairy black hole solutions) in Appendix F.

^bAlbeit shocks can form from smooth initial data for more “standard” matter fields, such as for perfect fluids.³⁷

Our notation is: the metric has $- + ++$ signature, lower-case Greek letters index spacetime tensor components, lower-case Latin letter index spatial tensor components, the Riemann tensor is $R^\alpha_{\mu\beta\nu} = \partial_\beta \Gamma^\alpha_{\mu\nu} - \dots$, “*l.o.t.*” means “lower order terms” in derivatives (for example $\partial_t^2 \phi + \partial_t \phi = \partial_t^2 \phi + \text{l.o.t.}$), and $\mathbb{P}[\dots]$ means take the principal part of a set of equations, (for example $\mathbb{P}[\partial_t^2 \phi + \partial_t \phi] = \partial_t^2 \phi$). We set $8\pi G = c = 1$.

2. Horndeski gravity

The Horndeski gravity theories consist of all classical field theories that have a tensor field $g_{\mu\nu}$, a scalar field ϕ , have only up to second order derivatives in the action, and which have second-order equations of motion.^{17–19} We write the Horndeski action as

$$S = \int d^4x \sqrt{-g} (\mathcal{L}_1 + \mathcal{L}_2 + \mathcal{L}_3 + \mathcal{L}_4 + \mathcal{L}_5), \quad (1)$$

where

$$\mathcal{L}_1 \equiv \frac{1}{2}R + X - V(\phi), \quad (2)$$

$$\mathcal{L}_2 \equiv \mathcal{G}_2(\phi, X), \quad (3)$$

$$\mathcal{L}_3 \equiv \mathcal{G}_3(\phi, X) \square \phi, \quad (4)$$

$$\mathcal{L}_4 \equiv \mathcal{G}_4(\phi, X) R + \partial_X \mathcal{G}_4(\phi, X) \delta_{\delta_1 \delta_2}^{\gamma_1 \gamma_2} \nabla_{\gamma_1} \nabla^{\delta_1} \phi \nabla_{\gamma_2} \nabla^{\delta_2} \phi, \quad (5)$$

$$\mathcal{L}_5 \equiv \mathcal{G}_5(\phi, X) G_{\mu\nu} \nabla^\mu \nabla^\nu \phi - \frac{1}{6} \partial_X \mathcal{G}_5(\phi, X) \delta_{\delta_1 \delta_2 \delta_3}^{\gamma_1 \gamma_2 \gamma_3} \nabla_{\gamma_1} \nabla^{\delta_1} \phi \nabla_{\gamma_2} \nabla^{\delta_2} \phi \nabla_{\gamma_3} \nabla^{\delta_3} \phi, \quad (6)$$

δ_{\dots} corresponds to the (generalized) Kronecker delta, and

$$X \equiv -\frac{1}{2}g^{\mu\nu} \nabla_\mu \phi \nabla_\nu \phi. \quad (7)$$

Following Papallo and Reall,⁴² we assume

$$\mathcal{G}_2(\phi, 0) = \partial_X \mathcal{G}_2(\phi, 0) = \mathcal{G}_3(\phi, 0) = \mathcal{G}_4(0, 0) = \mathcal{G}_5(0, 0) = 0. \quad (8)$$

to remove degeneracies between the various \mathcal{L} terms through field redefinitions $\phi \rightarrow f(\phi)$. The equations of motion are given by

$$E_{\mu\nu}^{(g)} \equiv -\frac{1}{\sqrt{-g}} \frac{\delta S}{\delta g^{\mu\nu}} = 0, \quad (9)$$

$$E^{(\phi)} \equiv -\frac{1}{\sqrt{-g}} \frac{\delta S}{\delta \phi} = 0. \quad (10)$$

We state the full equations of motion in Appendix A.

A special case of a Horndeski gravity is $4\partial ST$ (“4 derivative Scalar-Tensor”, alias “Einstein scalar Gauss-Bonnet”) gravity

$$S_{4\partial ST} \equiv \int d^4x \sqrt{-g} \left(\frac{1}{2}R + X - V(\phi) + \alpha(\phi)X^2 + \beta(\phi)\mathcal{R}_{GB} \right), \quad (11)$$

where $\mathcal{R}_{GB} \equiv R^2 - 4R_{\mu\nu}R^{\mu\nu} + R_{\mu\alpha\nu\beta}R^{\mu\alpha\nu\beta}$ is the Gauss-Bonnet scalar. While the Gauss-Bonnet scalar does not appear in the action (1), the equations of motion for $4\partial ST$ gravity are second order in time and spatial derivatives.^{30,31,43,44} In fact one can show through field redefinitions that the Gauss-Bonnet scalar term can be transformed into the form presented in Eq. (1).⁴⁵ This theory has attracted attention as for some coupling functions $\beta(\phi)$, black holes can have scalar hair.^{21,22,46–50}

Generically one may expect the scalar field ϕ to *conformally couple* to matter fields in the following way^{51,52}

$$S_{(M)} = \int d^4x \sqrt{-g} L_{(M)} [\Psi_{(M)}, A^2(\phi) g_{\mu\nu}], \quad (12)$$

where $L_{(M)}$ is the “matter Lagrangian”, $\Psi_{(M)}$ stands for all matter fields, and $A^2(\phi)$ is a positive definite function of ϕ . Through *Weyl transformations*^c, that is field redefinitions of the form $g_{\mu\nu} \rightarrow \Omega(\phi) \tilde{g}_{\mu\nu}$ one can redefine the metric to remove the factor A^2 (by choosing $\Omega = 1/A^2$), at the expense of adding a scalar field functional prefactor $1/A^2$ in front of the Ricci scalar in \mathcal{L}_1 , and having to redefine the other Horndeski functions \mathcal{G}_i ^d. If there no coupling of the scalar field to the Ricci scalar of the form $f(\phi)R$, the action is said to be in the *Einstein frame*.⁵⁴ If there is no conformal coupling between the metric and ϕ in the matter action, the action is said to be in the *Jordan frame*. For more discussion, see 55. This terminology was invented before the Horndeski theories became better known, so the Einstein and Jordan frames do not exhaustively describe all possible couplings such as those found in \mathcal{L}_4 and \mathcal{L}_5 . For more discussion about the Jordan and Einstein frames in the context of classical scalar-tensor gravity, see 51. The form of the coupling A can have a dramatic effect on the potential observational effects of a given theory.^{51,52,56,57}

Finally we mention that in fact one can have an even more general *disformal coupling* between the metric and scalar field,⁵⁸ which do not introduce any new degrees of freedom to the action:

$$S_{(M)} = \int d^4x \sqrt{-g} L_{(M)} [\Psi_{(M)}, A^2(\phi, X) (g_{\mu\nu} + B^2(\phi, X) \nabla_\mu \phi \nabla_\nu \phi)]. \quad (13)$$

Here A^2 and B^2 are positive functions of ϕ, X . While disformal couplings were proposed several decades ago,⁵⁸ they remain relatively less well studied than conformal couplings. Moreover, the Horndeski theories are not invariant under *disformal transformations*, that is field redefinitions of the form $g_{\mu\nu} \rightarrow A^2(\phi, X) (g_{\mu\nu} + B^2(\phi, X) \nabla_\mu \phi \nabla_\nu \phi)$. Under disformal transformations the Horndeski Lagrangian can transform to have terms that have higher than second order derivatives. New degrees of freedom are not necessarily introduced by these higher

^cWeyl transformations are also sometimes called *conformal transformations*, although we avoid that terminology here, as that can also refer to conformal coordinate transformations, where the coordinates themselves x^μ are transformed so that that $g_{\mu\nu} \rightarrow \Omega g_{\mu\nu}$.

^dWe note that in general a Weyl transformation will transform $4\partial ST$ gravity to a more general Horndeski gravity theory, due the transformation properties of the Gauss-Bonnet scalar.⁵³

derivative terms though; for more discussion see Refs. 59, 33. We note that the general form of the Horndeski gravity theories are preserved under *special disformal transformations*, that is transformations where A, B are only functions of ϕ .⁶⁰

3. Local well-posedness of the equations of motion

3.1. General considerations

Local well posedness of the equations of motion is necessary for constructing numerical solutions. For hyperbolic partial differential equations, the theory must have a well-posed *initial value problem* (IVP). For elliptic partial differential equations, the theory must have a well posed *boundary value problem* (BVP). A system of partial differential equations for a given problem setup are well posed if⁶¹

- (1) The problem has a solution
- (2) The solution is unique
- (3) The solution depends continuously on the given data for the problem (for example, for an initial value problem this would be initial data).

The last criteria is somewhat subtle, as continuity needs to be defined with respect to function space. A theory that has a well-posed IVP or BVP with respect to one function space may not be well posed in another^e.

As we review in Appendix B, the equations of motion for Horndeski gravity have a well-posed IVP provided they form a strongly hyperbolic system. As in GR,^{62, 64, 65} the hyperbolicity properties of the Horndeski equations of motion are formulation-dependent and gauge-dependent. By “formulation”, we mean the choice of evolution variables and how the equations of motion are written (for example, the BSSN formulation^{66, 67} and modified harmonic formulation^{68–70}), and by “gauge” we mean the choice of the four coordinate (gauge) degrees of freedom (for example, harmonic gauge⁷¹). The choice of a suitable formulation and gauge is called a *hyperbolic reduction*.⁶⁸

Since Choquet-Bruhat’s work on the Einstein equations in harmonic coordinates,⁷¹ many strongly-hyperbolic reductions of the Einstein equations have been found (for reviews, see 65, 62, 63). Perturbatively solving the Horndeski equations about GR also leads to well-posed evolution, as the principal part of the perturbative equations remain the same as for GR to all orders in perturbation theory. We discuss the perturbative method in more detail in Sec. 4.

Up until recently, it was unclear if it was possible to formulate a hyperbolic reduction of the full, general Horndeski equations of motion. Given the earlier success of the generalized harmonic formulation in evolving the Einstein equations^{3, 69, 70, 72} (under which the Einstein equations are strongly hyperbolic⁶⁸) Papallo and Reall in-

^eTypically well-posedness for PDE in physics are defined with respect to a *Sobolev space* such as H^2 , which is the space of all functions that have weak partial derivatives of at least second order that are square integrable (L^2); for more discussion see 61, 62, 63.

vestigated the hyperbolicity of the Horndeski equations in the generalized harmonic formulation. They found that for all but a small subset of the theories (in particular, those with $\mathcal{G}_4 = \mathcal{G}_5 = 0$), the equations of motion were only weakly, but not strongly hyperbolic.^{42,73} Recently though, Kovacs and Reall have introduced the *modified generalized harmonic* (MGH) formulation, in which Horndeski equations of motion do form a strongly hyperbolic system,^{30,31} provided the Horndeski terms in the solution are *weakly coupled*. Currently the MGH formulation is the only known strongly hyperbolic formulation for the full, general Horndeski equations of motion. Moreover, there are other strongly hyperbolic formulations of specific Horndeski gravity theories; see Sec. 5.

3.2. Weakly-coupled regime

Before continuing to the various hyperbolic reductions of the Horndeski equations, we first define what is meant by a weakly coupled solution. This condition demands that the smallest length scale as defined by the spacetime curvature is large compared to the length scales defined by the Horndeski coupling constants. The weak coupling condition has also been called the *weak background field* condition.⁴² We can make these conditions more concrete by considering an orthonormal basis $\{e_\mu\}$ (we assume we have also chosen a foliation of spacelike hypersurfaces $\{\Sigma_t\}$, and that the e_0 are chosen to be orthogonal to each $t = \text{const.}$ hypersurface). We define the function $M_t[T]$ as giving the magnitude of the largest component of a tensor T with respect to this basis on the leaf Σ_t , and define the length scales

$$M_t[R^\alpha{}_{\mu\beta\nu}] \equiv \frac{1}{L_R^2}, \quad M_t[\nabla_\mu\phi] \equiv \frac{1}{L_1}, \quad M_t[\nabla_\mu\nabla_\nu\phi] \equiv \frac{1}{L_2^2}. \quad (14)$$

We then define the shortest length scale as

$$\frac{1}{L} \equiv \max \left[\frac{1}{L_R}, \frac{1}{L_1}, \frac{1}{L_2} \right]. \quad (15)$$

The weak coupling condition is obeyed on a leaf Σ_t if the following conditions are obeyed

$$\frac{1}{L^{2k-2}} |\partial_X^k \mathcal{G}_2| \ll 1, \quad k = 1, 2 \quad (16a)$$

$$\frac{1}{L^{2k}} |\partial_X^k \partial_\phi^l \mathcal{G}_3| \ll 1, \quad k = 0, 1, 2, \quad l = 0, 1, \quad 1 \leq k + l \leq 2 \quad (16b)$$

$$\frac{1}{L^{2k}} |\partial_X^k \partial_\phi^l \mathcal{G}_4| \ll 1, \quad k = 0, 1, 2, 3, \quad l = 0, 1, 2, \quad k + l \leq 3 \quad (16c)$$

$$\frac{1}{L^{2k+2}} |\partial_X^k \partial_\phi^l \mathcal{G}_5| \ll 1, \quad k = 0, 1, 2, 3, \quad l = 0, 1, 2, \quad 1 \leq k + l \leq 3. \quad (16d)$$

From the Horndeski equations of motion (see Appendix A), we see these conditions imply that the Horndeski terms in the equations of motion are “small” compared to the shortest curvature/scalar gradient length scale. Solutions that are not weakly-coupled are called *strongly-coupled*. There is currently no consensus on how to interpret strongly-coupled solutions to the Horndeski gravity theories. Clearly, some

Horndeski gravity theories can have well-defined strongly coupled classical solutions (for a simple example: minimally coupled scalar fields in GR can be classically evolved up to the formation of curvature singularities⁷⁴). There are some Horndeski theories that appear to break down though in the strong coupling regime, such as $4\partial ST$ gravity with a nonzero Gauss-Bonnet coupling β .^{38,39,41,75–78} Whether or not a given Horndeski theory has sensible strongly-coupled solution will likely need to be determined on a case-by-case basis. We will largely restrict our discussion to weakly-coupled solutions in this article, although we will mention numerical work on solutions that exhibit the Vainshtein mechanism, which necessarily lies in the strongly-coupled regime.^{79,80} Note that black holes (and black hole mergers) can be in the weakly-coupled regime for a Horndeski gravity theory, so long as the curvature scale set by the black hole (such as the black hole radius) is large compared to the scale set by the Horndeski coupling constants. More generally, Horndeski solutions that describe gravity in the strong field, dynamical regime can also be weakly coupled so long as the Horndeski coupling constants are smaller than the smallest curvature scale set by the solution.

4. Local well-posedness of the *perturbative* equations of motion

We first consider the Horndeski equations of motion rewritten in a *naive perturbation theory* (or *order-reduction*) scheme. The main advantage of the naive-perturbative method is that it reduces the principal part of the Horndeski equations of motion to that of GR, so that methods already used in numerical relativity can be directly applied. The main disadvantage of the naive-perturbative approach is the presence for so-called *secular instabilities*, which can spoil the accuracy of higher order perturbative solutions that are integrated over sufficiently long time scales.

In the perturbative approach, the metric and scalar field are expanded as a power-series in a small parameter ϵ about a GR background

$$g_{\mu\nu} = g_{\mu\nu}^{(0)} + \sum_{k=1}^{\infty} \epsilon^k g_{\mu\nu}^{(k)}, \quad (17a)$$

$$\phi = \phi^{(0)} + \sum_{k=1}^{\infty} \epsilon^k \phi^{(k)}. \quad (17b)$$

Here ϵ is a dimensionless number; it is used to keep track of the perturbative order one is working in, and can be set to $\epsilon = 1$ before evaluating an expression at a given order. The expressions (17) are inserted into the full Horndeski equations of motion $E_{\mu\nu}^{(g)}$ and $E^{(\phi)}$ (see Appendix A), and truncated at each order in ϵ . This results in

a “tower” of partial differential equations, that schematically take the form

$$\begin{aligned} \epsilon^0 E_{\mu\nu}^{(g,0)} [g_{\mu\nu}^{(0)}, \phi^{(0)}] &= 0, & \epsilon^0 E^{(\phi,0)} [g_{\mu\nu}^{(0)}, \phi^{(0)}] &= 0, \\ &\vdots & & \\ \epsilon^k E_{\mu\nu}^{(g,k)} [g_{\mu\nu}^{(0)}, \phi^{(0)}, \dots, g_{\mu\nu}^{(k)}, \phi^{(k)}] &= 0, & \epsilon^k E^{(\phi,k)} [g_{\mu\nu}^{(0)}, \phi^{(0)}, \dots, g_{\mu\nu}^{(k)}, \phi^{(k)}] &= 0, \end{aligned} \quad (18)$$

$$\vdots \quad (19)$$

Moreover, we assume that each Horndeski term (beyond \mathcal{L}_1) appears at least at order ϵ

$$\mathcal{L}_{i \geq 2} \sim \epsilon^{p_i}, \quad p_i \geq 1. \quad (20)$$

This is easy to accomplish by for example setting the couplings constants to be $\sim \epsilon^{p_i}$. We note that this is a distinct condition from a solution to the Horndeski theories being weakly coupled (see Eq. (16)). From Eqs. (17), (20), the principal part of the perturbative equations of motion (18), to every order in k , is the same as the principal part of GR (the \mathcal{L}_1 term). This can be seen by consider the full Horndeski equations of motion, which given Eq. (20) take the form

$$\begin{aligned} \left(E^{(g)} \right)_{\beta}^{\alpha} &= -\frac{1}{4} \delta_{\beta}^{\alpha} \gamma_1 \gamma_2 R_{\gamma_1 \gamma_2}^{\delta_1 \delta_2} - (V + X) \delta_{\beta}^{\alpha} - \nabla^{\alpha} \phi \nabla_{\beta} \phi + \mathcal{O}(\epsilon^p) \\ &\equiv \left(E_{GR}^{(g)} \right)_{\beta}^{\alpha} + \mathcal{O}(\epsilon^p), \end{aligned} \quad (21)$$

$$\begin{aligned} E^{(\phi)} &= -\square \phi + \partial_{\phi} V + \mathcal{O}(\epsilon^p) \\ &\equiv E_{GR}^{(\phi)} + \mathcal{O}(\epsilon^p). \end{aligned} \quad (22)$$

To each order in k , the principal part for the evolved variables $g_{\mu\nu}^{(k)}, \phi^{(k)}$ is the same as it is for GR. Plugging in (17), to each order in k we have

$$\left(E_{GR}^{(g)} [g_{\mu\nu}^{(k)}, \phi^{(k)}] \right)_{\beta}^{\alpha} + \left(F^{(k)} [g_{\mu\nu}^{(0)}, \phi^{(0)}, \dots, g_{\mu\nu}^{(k-1)}, \phi^{(k-1)}] \right)_{\beta}^{\alpha} = 0, \quad (23)$$

$$E_{GR}^{(\phi)} [g_{\mu\nu}^{(k)}, \phi^{(k)}] + F^{(\phi)} [g_{\mu\nu}^{(0)}, \phi^{(0)}, \dots, g_{\mu\nu}^{(k-1)}, \phi^{(k-1)}] = 0, \quad (24)$$

where $\left(F^{(g,k)} \right)_{\beta}^{\alpha}$ and $F^{(\phi,k)}$ contain only up to first derivatives of their arguments. The perturbative equations of motion to each order in k can then be evolved in a well-posed manner using the same formulations of the equations of motion used in numerical evolutions of the Einstein equations.

A common assumption is to set $\phi^{(0)} = 0$, and to solve only the first order corrections to the equations of motion. From the Horndeski equations of motion and using the conditions (8), we see that with $\phi^{(0)} = 0$ then there are no corrections to the linearly corrected Einstein (tensor) equations $E_{\mu\nu}^{(g,1)}$ (assuming $V(0) = 0$), in which case we can set $g_{\mu\nu}^{(1)} = 0$. The linearly corrected scalar equations $E^{(\phi,1)}$ then only contain $\phi^{(1)}$ (and not $g_{\mu\nu}^{(1)}$), so we can solve for the scalar field on a GR background. This approach is often called the *decoupling approximation*. The

scalar field back-reaction on the metric appears at second order in the perturbative expansion^f.

The naive-perturbative approach has been applied to some Horndeski gravity theories.^{81–83} One of the most attractive features though of the formalism is that it can be applied to essentially any modified theory of gravity, including theories whose exact equations of motion may not have well-posed initial value formulations, such as *dynamical Chern-Simons gravity*^{10,84–88} and other higher derivative modified gravity theories.^{89,90} As discussed in Sec. 7.4, the presence of secularly growing error terms can complicate the interpretation of higher order perturbative solutions. In that section we discuss how the recently proposed *dynamical renormalization group* could potentially address the problem of secular growth in perturbative numerical solutions.

5. Local well-posedness of the *exact* equations of motion

We next consider well-posed formulations of the exact equations of motion for the Horndeski theories of gravity; that is for the complete set of equations listed in Appendix A. While exact solutions do not suffer from secular instabilities, one has to contend with finding a well-posed formulation of the equations of motion. We review well-posed formulations for various special cases of the Horndeski gravity theories, then end with a formulation that leads to well-posed evolution for all of the Horndeski gravity theories: the *modified generalized harmonic* (MGH) formulation.^{30,31}

5.1. Well posed formulations of quadratic Horndeski gravity

Quadratic Horndeski gravity (also often called “K-essence” theory^{91,92}), has the action

$$S = \int d^4x \sqrt{-g} (\mathcal{L}_1 + \mathcal{L}_2). \quad (25)$$

The equations of motion for this theory are given in Appendix A, (setting $\mathcal{G}_i = 0, i > 2$):

$$R_{\mu\nu} - \frac{1}{2}g_{\mu\nu}R + \frac{1}{2}\partial_X\mathcal{G}_2\nabla_\mu\phi\nabla_\nu\phi - \frac{1}{2}g_{\mu\nu}\mathcal{G}_2 = 0, \quad (26)$$

$$\nabla_\mu(\partial_X\mathcal{G}_2\nabla^\mu\phi) + \partial_\phi\mathcal{G}_2 = 0. \quad (27)$$

For this theory, the principal part of the tensor equation remains unchanged from that of GR, and it is straightforward to see that the scalar equations of motion remain strongly hyperbolic in the weak-coupling limit (see Ref. 93 for a more general discussion). Thus, the standard formulations used in numerical relativity can be used to evolve this class of Horndeski gravity theories (if shocks form in the equations of motion, high resolution shock capturing methods can be used,⁹⁴ see Sec. 7.3).

^fThe correction to the metric *will* generally occur at least at second order in the perturbative expansion, due to the presence of X in \mathcal{L}_1 .

5.2. Well-posed formulation of Cubic Horndeski gravity

We next consider cubic Horndeski gravity, which has the action

$$S = \int d^4x \sqrt{-g} (\mathcal{L}_1 + \mathcal{L}_2 + \mathcal{L}_3). \quad (28)$$

The equations of motion for this theory are given in Appendix A (setting $\mathcal{G}_i = 0, i > 3$). Kovacs²⁸ pointed out that from the perspective of local well-posedness in the weakly-coupled limit, the terms that could cause problems compared to GR are $R_{\alpha\beta}\nabla^\alpha\nabla^\beta\phi$ in the scalar equations of motion, and terms involving second derivatives of the scalar field in the tensor equations of motion. The Ricci tensor can be replaced with second derivatives of the scalar field by considering the trace-reversed tensor equations of motion

$$\begin{aligned} E_{\alpha\beta}^{(g)} - \frac{1}{2}g_{\alpha\beta}g^{\mu\nu}E_{\mu\nu}^{(g)} &= R_{\mu\nu} \\ &+ \frac{1}{2}(\mathcal{G}_2 - X\partial_X\mathcal{G}_2 - X\partial_X\mathcal{G}_3\Box\phi)g_{\alpha\beta} \\ &- \frac{1}{2}(1 + \partial_X\mathcal{G}_2 + 2\partial_\phi\mathcal{G}_3)\nabla_\alpha\phi\nabla_\beta\phi \\ &+ \frac{1}{2}\partial_X\mathcal{G}_3(-\Box\phi\nabla_\alpha\phi\nabla_\beta\phi + 2\nabla_{(\alpha}\phi\nabla_{\beta)}\nabla_\gamma\phi\nabla^\gamma\phi). \end{aligned} \quad (29)$$

Using this to replace $R_{\mu\nu}$ in the scalar equation of motion, the principal symbol for the tensor and scalar field takes an upper triangular structure (see Kovacs²⁸ for the full equations of motion). With this simplified structure, Kovacs was able to prove the local well-posedness of cubic Horndeski gravity for three popular formulations used in numerical relativity, including the BSSN formulation^{66,67} and the CCZ4 formulation^{95,96} of the equations of motion. As we review later, one of these formulations has been used to evolve (binary) black holes in this theory.^{40,97}

5.3. Well-posed formulations of Bergmann–Wagoner scalar-tensor gravity theories

For completeness, we also mention the original *scalar-tensor* gravity theories^{52,98–100}

$$S = \int d^4x \sqrt{-g} (F(\phi)R + Z(\phi)X - V(\phi)). \quad (30)$$

When $F = \phi, Z = \omega/\phi$ (where ω is a constant), and $V = 0$, this action reduces to Brans-Dicke gravity¹⁰¹ (in this case the theory limits to GR when $\phi \rightarrow 1, \omega \rightarrow \infty$). Scalar-tensor gravity is a special case of the \mathcal{L}_1 , \mathcal{L}_2 , and \mathcal{L}_4 Horndeski gravity terms: $\mathcal{L}_2 = (Z(\phi) - 1)X$, $\mathcal{L}_4 = F(\phi) - 1$, This theory was shown to have a well-posed initial value formulation in a BSSN-styled formulation of the theory¹⁰² (although note that the authors in that work defined their scalar field differently from what we have presented here). Provided there is no coupling of the form $A^2(\phi)g_{\mu\nu}$ in the matter Lagrangian, the action (30) is said to be in the *Jordan frame*. One can generally perform a Weyl transformation (a field redefinition of the

form $g_{\mu\nu} \rightarrow \Omega(\phi) \tilde{g}_{\mu\nu}$) to set $F(\phi) R \rightarrow \tilde{R}$; that is to go to the *Einstein frame* (see for example Ref. 51). In this frame, there is no mixing between the scalar and tensor degrees of freedom in the principal symbol. The well posedness of the equations of motion in the Einstein frame is then straightforward to show, and the theory can essentially be solved numerically using the same methods that are used to solve for the GR with a minimally coupled scalar field with a potential. Because of this, most researchers in numerical relativity evolve black holes and neutron stars in the Einstein frame; recent work includes 103, 104, 94.

5.4. A well-posed formulation for all Horndeski gravity theories: the modified generalized harmonic (MGH) formulation

There is currently only one known strongly hyperbolic formulation for general weakly-coupled Horndeski gravity theories (\mathcal{L}_1 through \mathcal{L}_5): the *modified generalized harmonic (MGH) formulation*^{30,31g}. The setup for the formulation is: in a Lorentzian spacetime (M, g) , we introduce two auxiliary Lorentzian metrics $\tilde{g}^{\alpha\beta}$ and $\hat{g}^{\alpha\beta}$. We will always raise and lower indices with the spacetime metric $g_{\alpha\beta}$, so for example $\hat{g}^{\alpha\beta} \equiv g^{\alpha\gamma} g^{\beta\delta} \hat{g}_{\gamma\delta}$. We also define the traces $\tilde{g} \equiv \tilde{g}^{\alpha\beta} g_{\alpha\beta}$ and $\hat{g} \equiv \hat{g}^{\alpha\beta} g_{\alpha\beta}$. The MGH formulation imposes the following conditions on the coordinate functions x^γ :

$$\begin{aligned} C^\gamma &\equiv H^\gamma - \tilde{g}^{\alpha\beta} \nabla_\alpha \nabla_\beta x^\gamma \\ &= H^\gamma + \tilde{g}^{\alpha\beta} \Gamma_{\alpha\beta}^\gamma \dot{=} 0. \end{aligned} \quad (31)$$

We put a “dot” over the last equals sign to indicate that numerically, one generally expects C^γ to not exactly equal zero due to truncation error. As in the generalized harmonic formulation,^{68,69,72} H^γ are the source functions that, along with $\tilde{g}^{\alpha\beta}$ and $\hat{g}^{\alpha\beta}$, specify the gauge, and C^γ is called the *constraint violation*. We next define the MGH equations of motion as

$$\begin{aligned} \left(E^{(g, MGH)} \right)^{\alpha\beta} &\equiv \left(E^{(g)} \right)^{\alpha\beta} - \hat{P}_\delta^{\gamma\alpha\beta} \nabla_\gamma C^\delta \\ &\quad - \frac{1}{2} \kappa (n^\alpha C^\beta + n^\beta C^\alpha + \rho n^\gamma C_\gamma g^{\alpha\beta}) = 0, \end{aligned} \quad (32)$$

where n^α is a time-like vector (we assume n^α is timelike with respect to $g^{\alpha\beta}$, $\tilde{g}^{\alpha\beta}$, and $\hat{g}^{\alpha\beta}$), and

$$\hat{P}_\delta^{\gamma\alpha\beta} \equiv \frac{1}{2} (\delta_\delta^\alpha \hat{g}^{\beta\gamma} + \delta_\delta^\beta \hat{g}^{\alpha\gamma} - \delta_\delta^\gamma \hat{g}^{\alpha\beta}). \quad (33)$$

In Eq. (32) we included constraint damping terms with the constants κ and ρ ; see 106. These terms would not affect the solution if C^γ was exactly zero, but in numerical applications this is generally not the case, and without damping terms

^gNote added after publication: the MGH formulation has been adapted to the CCZ4 formulation by Aresté, Clough, and Figueras.¹⁰⁵ In that work the authors also evolved binary black holes through merger in 4DST gravity, using singularity-avoiding coordinates.

the constraint violation could blow up exponentially in time.^{3,70,72,107} ^h From Eq. (31), we see that in the MGH formulation the coordinates x^α obey a hyperbolic equation with characteristics determined by $\tilde{g}^{\alpha\beta}$. Taking the divergence of Eq. (32), and assuming $\nabla_\alpha E^{\alpha\beta} = 0$ (which by general covariance of the action, holds for the Horndeski equations of motion), we obtain a hyperbolic equation for the constraint violating modes C^α :

$$\begin{aligned} -\frac{1}{2}\hat{g}^{\alpha\gamma}\nabla_\alpha\nabla_\gamma C^\beta - \hat{g}^{\gamma\beta}R_{\delta\gamma}C^\delta - (\nabla_\alpha\hat{P}_\delta{}^{\gamma\alpha\beta})(\nabla_\gamma C^\delta) \\ -\frac{1}{2}\kappa\nabla_\alpha(n^\alpha C^\beta + n^\beta C^\alpha + \rho n^\gamma C_\gamma g^{\alpha\beta}) = 0. \end{aligned} \quad (34)$$

From Eq. (34), we see that the constraint violating modes obey a hyperbolic equation with characteristics determined by $\tilde{g}^{\alpha\beta}$.

Kovacs and Reall proved that in the weak coupling regime that the Horndeski equations of motion in the MGH formulation:

$$\left(E^{(g, MGH)}\right)^{\mu\nu} = 0, \quad E^{(\phi)} = 0, \quad (35)$$

form a strongly hyperbolic system of partial differential equations.^{30,31} Specifying a gauge in the MGH formulation amounts to choosing the functional form of $\tilde{g}^{\alpha\beta}$, $\hat{g}^{\alpha\beta}$, and H^γ . With the choice $\tilde{g}^{\alpha\beta} = \hat{g}^{\alpha\beta} = g^{\alpha\beta}$, the MGH formulation reduces to the generalized harmonic formulation.

We next outline the main elements of Kovacs and Reall's strong hyperbolicity argument. In the GH formulation, the coordinate degrees of freedom and the constraint violation degrees of freedom all have the same characteristics: they are determined by $g^{\mu\nu}$. The equations of motion for GR with minimally coupled matter fields in the GH formulation are remarkable as despite the degeneracy of the eigenvalues of the principal symbol, the principal symbol is diagonalizable. This is not the case of the Horndeski gravity theories: as Papallo and Reall showed,^{42,73} there remains a Jordan block in the principal symbol of the equations of motion for these theories, that is locally the principal symbol takes the form

$$\mathcal{P}^{(GH)}(\xi) = \begin{pmatrix} c_1 & 0 & 0 & \cdots \\ 0 & c_1 & 0 & \cdots \\ 0 & 0 & \ddots & \\ \cdots & 0 & c_n & 1 \\ \cdots & 0 & 0 & c_n \end{pmatrix}, \quad (36)$$

where the c_i are the characteristic speeds. Papallo and Reall found this Jordan block cannot be removed for a single constraint violating mode. One of the key insights of Kovacs and Reall was to notice that the coordinates and constraint

^hNote that Eq. (32) is slightly different from Kovacs and Reall.³¹ Here we use $\nabla_\gamma C^\delta$ instead of $\partial_\gamma C^\delta$. We choose this form so that the MGH equations we introduce here matches that of the standard generalized harmonic formulation¹⁰⁷ in the limit $\hat{g}^{\alpha\beta} = \tilde{g}^{\alpha\beta} = g^{\alpha\beta}$.

violation fields did not need to propagate on the spacetime metric, as they are unphysical. The introduction of the auxiliary metrics $\tilde{g}^{\mu\nu}$ and $\hat{g}^{\mu\nu}$ breaks some of the degeneracies in the characteristic speeds in the principal symbol among the coordinate and gauge-violating degrees of freedom, which they showed is sufficient to make the principal symbol diagonalizable, at least for weakly-coupled solutions.^{30,31} To gain some intuition as to how breaking degeneracies in the eigenvalues of the principal symbol could help, recall that perturbing the eigenvalues of a Jordan-form matrix generally makes it diagonalizable, for example

$$\begin{pmatrix} c_n & 1 \\ 0 & c_n + \epsilon \end{pmatrix} \quad (37)$$

is diagonalizable with eigenvectors $(1, 0)$ and $(1, \epsilon)$.

The work of Kovacs and Reall suggests that it should be possible to generalize other formulations used to evolve the Einstein equations, for example the BSSN formulation of the equations of motion,^{66,67} to give a strongly hyperbolic formulation for the Horndeski equations of motion for weakly-coupled solutions.

6. Exact solutions to the *fixed* equations of motion

A related method to solving the full Horndeski equations is to modify (*fix*) the Horndeski equations in such a way that may allow for a well-posed initial value problem, even outside the weak-coupling regime. The *equation-fixing* method takes inspiration from the so-called Israel-Stewart method^{108–110} to render the relativistic Navier-Stokes equations into a strongly-hyperbolic system of equations.^{25,26} Fixing the equations involves modifying them in such a way so that only high-energy degrees of freedom are modified, and the dynamics of low-energy degrees of freedom remain essentially unchanged. If we view the equations of motion of Horndeski theory as describing a low-energy effective deviation from the Einstein equations, then the essential physics of the theory should be captured by the low-energy degrees of freedom anyways. Moreover, hyperbolicity/ellipticity is defined with respect to the principal part, which is most sensitive to high-frequency (high-energy) degrees of freedom, so changing that part of the equations of motion may render them strongly hyperbolic.

Fixing the equations may allow for a strongly hyperbolic reduction even for strongly coupled solutions (although, as mentioned earlier, this regime may lie outside the regime of applicability of the theory). To illustrate the idea of fixing in this situation, consider the scalar equations of motion for quadratic Horndeski gravity

$$\partial_0 (\sqrt{-g} \partial_X \mathcal{G}_2 \partial^0 \phi) + \partial_i (\sqrt{-g} \partial_X \mathcal{G}_2 \partial^i \phi) + \partial_\phi \mathcal{G}_2 = 0. \quad (38)$$

These equations can break down outside of the weak-coupled regime;^{111,112} one proposed way to prevent this breakdown is to fix the equations by introducing a

new field Π such that the equations of motion are¹⁰⁴

$$\partial_0 (\sqrt{-g}\Pi\partial^0\phi) + \partial_i (\sqrt{-g}\Pi\partial^i\phi) + \partial_\phi \mathcal{G}_2 = 0, \quad (39a)$$

$$\partial_0 \Pi + \frac{1}{\tau} (\Pi - \partial_X \mathcal{G}_2) = 0, \quad (39b)$$

where $\tau > 0$ is a new constant, which can be thought of as a “relaxation timescale”. Provided τ is shorter than the physical timescales that are being simulated, the “low-energy mode” of the solutions to the fixed system (39) should be similar to those of the full system (38). This fix has been found to be helpful for evolving outside of the weakly-coupled regime in the numerical evolution of this class of theories.^{94, 104, 113}

Beyond quadratic Horndeski gravity, this method has been applied to cubic Horndeski,¹¹⁴ and ESGB gravity.¹¹⁵ The fixing approach has also be applied to higher-derivative theories of gravity.^{26, 90} Much work remains in systematizing this approach, and quantitatively determining how much a given “fix” affects low-energy degrees of freedom in a given physical scenario (such as during black hole merger). There has not yet been any formal investigation of the well-posedness of the fixed Horndeski evolution and constraint equations. While it is reasonable to assume that the breakdown in hyperbolicity of a Horndeski theory indicates that the theory is no longer predictive in that regime (at least without including higher order corrections or a complete theory of say quantum gravity), there is some debate on how to interpret the breakdown.^{77, 78}

7. Challenges to constructing global solutions to Horndeski theories

7.1. Local versus global solutions

As we discussed in Sec. 3 and Sec. 5, for weakly-coupled solutions to the equations of motion, the structure of the equations of motion for the Horndeski are similar to the structure of the Einstein equations, and there exists several strongly hyperbolic formulations of the Horndeski equations of motion which have already been used in numerical relativity simulations of binary black hole spacetimes.^{41, 97, 107} While the Horndeski theories have a well-posed initial value problem in this regime, there is no guarantee that weakly coupled initial data will remain weakly coupled at later times.

We first recall that solutions to GR can break down at *spacetime singularities*.¹¹⁶ *Naked singularities* are not hidden by an event horizon. Naked singularities can be formed in Einstein gravity with a minimally coupled scalar field¹¹⁷ (and even in vacuum GR in four and higher¹¹⁸ dimensions) starting from regular, low-curvature initial data. This being said, these solutions are “unstable”,¹¹⁹ in the sense that small perturbations to the initial data lead to solutions where there are no naked singularities. More generally, the *weak cosmic censorship conjecture*¹²⁰ posits that for generic initial data, solutions to GR coupled to “standard” matter fields (for

example minimally coupled scalar field matter) have well defined global solutions (e.g. the spacetime is geodesically complete) outside of trapped regions. While there remains no proof of this conjecture, no counterexample to it has ever been found, and it is widely expected to be true.¹²¹ A well-defined solution can mean there are no curvature singularities outside of black hole horizons, but more broadly it can be taken to mean that the Einstein equations can be evolved in time, for all time and space, without having to introduce new (ad-hoc) boundary conditions.

Depending on the theory being considered, exact solutions to a Horndeski theory can suffer from several different kinds of issues.

- (1) For some Horndeski gravity theories, the equations of motion can lose their hyperbolic character in regions of high curvature—that is *elliptic regions*^{38–40} can form.
- (2) There is some evidence that curvature singularities can form outside of trapped region for some Horndeski theories.^{21, 46, 48, 49, 122, 123}
- (3) Some Horndeski gravity theories have solutions that form infinitely steep gradients, that is *shocks* or *caustics*^{111–113, 124–126} can form, even from smooth initial data. We note that shocks can form in perfect-fluid solutions to the Einstein equations, so strictly speaking this phenomenon is not entirely novel in the context of relativistic physics. Moreover, provided the equations of motion can be formulated as a conservative set of PDE, shock formation does not necessarily signal the breakdown of the theory.

Only strongly-coupled solutions to some Horndeski theories have been found to have these features, although there has been no exhaustive search of all solutions to all Horndeski theories. There is some numerical evidence that all of the above listed phenomena can form from initially weakly-coupled initial data. This being said, researchers have numerically evolved binary black hole spacetimes in quadratic Horndeski gravity, cubic Horndeski gravity, and in ESGB gravity (the last two theories which can form naked elliptic regions in gravitational collapse^{27, 38–40, 113}) through merger, and have found sets of initial data that did not lead to the formation of a naked elliptic regions or shocks.^{41, 97, 107}

Numerical studies of the detailed PDE nonlinear properties of the Horndeski gravity theories have mostly been confined to spherically symmetric spacetimes. In Fig. 1 we show several schematic Penrose diagrams that summarize the kinds of behavior that have been observed in spherical gravitational collapse of several Horndeski gravity theories. All curvature singularities and sonic lines that have been found in Horndeski gravitational collapse are spacelike, although given the difficulty of numerically evolving near those points, new simulations may reveal that the boundary between regular and irregular evolution may be null. A timelike boundary at a curvature singularity or sonic line would lead to ill-posed evolution, unless suitable boundary conditions could be found for that boundary region, or if that region was excised along a null ray.

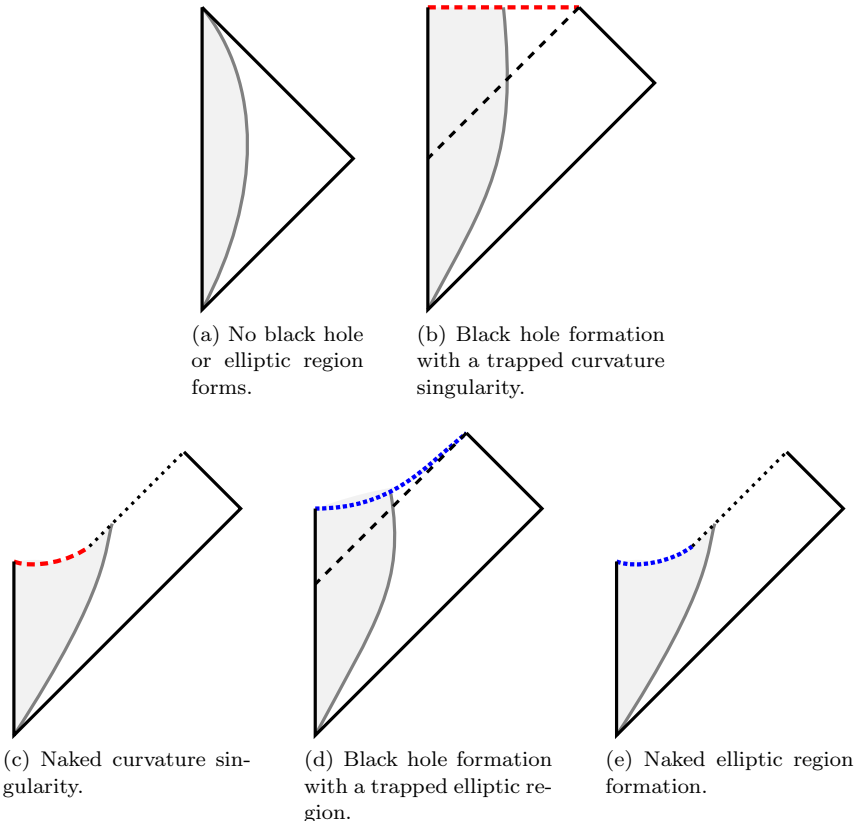


Fig. 1. Schematic Penrose diagram of the different kinds of spherical gravitational collapse that have been observed in Horndeski theories, starting from weak-field initial data with no initial black hole. The gray shaded region depicts the region where there is a nonzero scalar field value ϕ , that is we depict gravitational collapse that is driven by the Horndeski scalar field. A black dashed line indicates the location of an event horizon, and the black dotted line indicates a region that would need to be excised from the numerical domain in order to maintain well-posed evolution in an untrapped region. A red dashed line indicates a curvature singularity, while a blue dotted line indicates a sonic line. Panels (1a) and (1b) describe collapse that has been observed in GR coupled to “standard” matter fields and some Horndeski gravity theories. Other Horndeski gravity theories, such as variants of ESGB gravity and cubic Horndeski gravity theory, can form (naked) curvature singularities and (naked) elliptic regions.^{38–41,75–78,97} The formation of either signals the solution has exited the weakly-coupled regime. It is worth noting that clearly not all Horndeski theories will form elliptic regions, for example GR with minimally coupled scalar field is a Horndeski gravity theory.

Some caveats about Fig. 1: during a numerical evolution, quasi-local definitions of horizons (such as the apparent horizon) are typically used to locate the surface of black holes.¹²⁷ Black hole apparent horizons are located inside event horizons so long as the Null Convergence Condition ($R_{\mu\nu}k^\mu k^\nu \geq 0$ for all null vectors k^μ) holds,¹¹⁶ but this condition does not hold for many Horndeski gravity theories, even within the weakly-coupled regime. For example the black hole horizon can shrink with the growth of scalar hair in $4\partial ST$ gravity.^{39, 41, 75, 76, 107} Because of this, there is generally no guarantee within Horndeski gravity that an elliptic region contained within an apparent horizon will remain within one for all times, although empirically this does appear to be the case for solutions that are sufficiently weakly coupled exterior to all black hole horizons^{39–41, 75, 76, 97, 107} (for a recent discussion about different notions of horizons in the Horndeski gravity theories, see 36). Another subtlety is that the characteristic speeds of some degrees of freedom in Horndeski gravity can travel faster than the speed of light as determined by the spacetime lightcones,¹²⁸ although in principle this can be accounted for by suitably generalizing the notion of a horizon.³⁶

Finally, we mention that order-reduced solutions to the Horndeski theories only suffer from one potential problem not present in solutions to GR: errors can grow secularly over time. This can be a problem for accurately evolving binary black hole/neutron star spacetimes over many orbits. The issue of the *secular growth* of errors is generic to ordinary perturbation theory, and can be addressed using *renormalization group* methods, which have yet though to be implemented in numerical relativity codes.

7.2. *Exact equations: failure of hyperbolicity in the strongly-coupled regime*

Strong/weak hyperbolicity in the weakly-coupled regime is formulation-dependent and gauge-dependent. In the strongly coupled regime, the hyperbolicity of some Horndeski theories can fail in a more dramatic way: the equations of motion can develop fundamentally elliptic degrees of freedom. More formally, the equations of motion for many Horndeski gravity theories form a system of *mixed-type* partial differential equations. The mixed-type property of the Horndeski equations of motion sets them apart from the other PDE of classical physics: the Einstein equations of GR, the Maxwell equations of Electrodynamics, the Euler equations of fluid dynamics, or the classical equations of motion for the standard modelⁱ. Those equations of motion for those theories are always hyperbolic in a Lorentzian spacetime.

The model equations for mixed-type behavior are the Tricomi and Keldysh equa-

ⁱWe note though in rotating frames of reference that the classical wave equation becomes a mixed-type equation. This behavior is not an *inherent* property of the classical wave equation though: it simply reflects a particular choice of coordinates. For more discussion see Ref. 129

tions,^{130,131} which respectively are

$$\partial_x^2 u + x \partial_y^2 u = 0, \quad \partial_x^2 u + \frac{1}{x} \partial_y^2 u = 0. \quad (40)$$

These equations are hyperbolic when $x < 0$, parabolic when $x = 0$, and elliptic when $x > 0$. The characteristic speeds in the Keldysh equation blow up before reaching the elliptic region; thus instabilities may appear in a code before reaching the elliptic region because of the Courant-Friedrich-Lowy condition being violated in explicit time-stepping codes. By contrast, the characteristic speeds remain bounded up until the formation of the elliptic region for the Tricomi equation. The boundary between the elliptic and hyperbolic region of a mixed-type equation is called the *sonic line*.^{132,133} We provide a brief, more general review of mixed-type equations in Appendix C.

Given that black holes in GR are expected to generically have curvature singularities in their interior,¹³⁴ it is generally expected that black hole solutions to the Horndeski gravity theories will become strongly coupled deep enough inside the hole. In general agreement with this, sonic lines have been found to occur inside and outside of black hole horizons for several different Horndeski theories; whether the region appears inside or outside of a horizon depends on the relative size of the Horndeski terms in the action, and the strength of the spacetime curvature outside the black hole horizon.^{27,38–41,75,76} Black hole excision has been applied to evolve black holes in 4 ∂ ST gravity^{41,107} to excise the elliptic region. Black holes in Cubic Horndeski gravity theories have also been evolved using puncture-like coordinates *without* using black hole excision, by adiabatically setting to zero the Horndeski coefficients inside the black hole horizon^{40,97} (thus the theory in some sense adiabatically reduces to GR inside the black hole)—we note that the authors refer to this scheme also as a form of “excision”. Sonic lines have been found in solutions to quadratic Horndeski gravity theories as well.^{27,113,135}

Recent work by Barausse et. al. have suggests that the elliptic regions found in the solution to some quadratic Horndeski gravity theories could be removed with a suitable choice of gauge,⁹⁴ at least for spherically symmetric evolution of the theory. It seems unlikely that elliptic regions could be removed for solutions to all Horndeski theories, although there is no rigorous proof that is the case.

Mixed-type problems appear in, for example fluid mechanics,^{136,137} and even in some numerical relativity applications (namely: when studying hyperbolic equations in a rotating frame of reference).¹²⁹ Given these previous applications, some numerical methods have been developed and successfully employed to solve mixed-type PDE across a sonic line.^{129,138,139} In principle then, it may be possible to solve the Horndeski equations of motion beyond the sonic line into the elliptic region. These solutions are likely to be of little physical interest though, as the formation of the sonic line essentially signals the breakdown of the weak-coupling regime of the solution at hand.

7.3. Exact equations: shock/caustic formation

The model equation for shock formation is Burgers' equation^{140, 141}

$$\partial_t u + \frac{1}{2} \partial_x (u^2) = 0. \quad (41)$$

This equation is *genuinely nonlinear*, that is the characteristic speed is a non-constant function of the field u itself^{1, 37, 61, 142} (in this case, the characteristic speed $c = u$). Similarly to Burgers' equation, the equations of motion for some Horndeski theories can also be genuinely nonlinear.¹²⁵ Shock formation for smooth initial data has been studied in particular detail for quadratic-Horndeski gravity theories (k-essence).^{111, 126, 135, 143}

We note that shock formation can occur even in vacuum GR, namely “gauge-shocks” can form from smooth initial data.^{144–147} Unlike in GR, shocks can form from smooth initial data for k-essence regardless of the gauge/formulation used, at least in 1 + 1 dimensional setups.^{111, 125} It is likely that it will be more difficult to form shocks in 3 + 1 asymptotically flat evolution as compared to 1 + 1 evolution due to the effect of dispersion, although further work will be needed in this direction to determine how prevalent shocks are in different subsets of Horndeski gravity.

Even when shocks do form, in principle it is possible to (numerically) solve the Horndeski theories by formulating the shock front as a *Riemann problem*,^{37, 148} provided one writes the Horndeski equations of motion as a system of conservation laws, that is into a system of the form³⁷

$$\partial_0 \left(\sqrt{h} \mathbf{U} \right) + \partial_i \left(\sqrt{h} \mathbf{F}^i \right) = \mathbf{S}, \quad (42)$$

where \mathbf{U} is the vector of conserved variables, \mathbf{F}^i are the vector of flux functions, \mathbf{S} is the vector of source terms, and we have used the 3 + 1 decomposition (49). Once a set of equations has been written in conservative form, a numerical method typically finds a *weak solution* to solve the equations through shocks. Conservation laws can have multiple weak solutions; picking the “physical” one can require a detailed knowledge of the PDE properties of the equations of motion. As one example, for the Burgers equation ((41); or more generally the Euler equations of fluid dynamics) one can introduce an *entropy condition*, and the physical weak solution is then the entropy increasing solution.¹⁴⁸

Some work has been done to successfully numerically evolve the equations of motion for some quadratic Horndeski (K-essence) theories using shock-capturing methods, including in the inspiral and collision of binary neutron stars with k-essence with the equations of motion written in a conservative form.^{94, 103, 104, 135} This being said, other Horndeski theories may suffer a breakdown in hyperbolicity (see Sec. 7.2), before a shock can form. The study of weak solutions to the Horndeski equations has not been thoroughly studied.

7.4. Perturbative solutions: secular instabilities, and the numerical dynamical renormalization group

The main technical challenge to using naive perturbation theory (Sec. 4) for long-time evolution is that in this approach, errors can grow secularly in time.¹⁴⁹ The problem can be illustrated with the following perturbed simple harmonic oscillator:

$$\frac{d^2u}{dt^2} + \omega^2 u + \epsilon \frac{d^2u}{dt^2} = 0, \quad u(0) = 0, \quad u'(0) = \omega. \quad (43)$$

Here ω is a constant and $\epsilon \ll 1$. The solutions order-by-order in ϵ are

$$u^{(0)}(t) = \sin(\omega t), \quad (44a)$$

$$u^{(1)}(t) = \frac{1}{2}\epsilon(\sin(\omega t) - t\omega \cos(\omega t)), \quad (44b)$$

⋮

The presence of $t\omega \cos(\omega t)$ signals the existence of a secular instability (the full solution is $u(t) = (1 + \epsilon) \sin(\omega t / (1 + \epsilon))$). Solving to higher orders in ϵ perturbatively will only introduce higher powers of t in the solution.

Several methods have been developed to address this secular growth of error (such as the method of multiple scales^{149,150}); most of these method have been shown to be special cases of a more general method call the *dynamical renormalization group* (DRG).^{151–154} Operationally speaking, the essence of the DRG is promote the constants of the background solution to dynamical functions, which are chosen to cancel out the secularly growing terms in the solution to a given perturbative order. In the case of the perturbed simple harmonic oscillator, the amplitude A and frequency ω of the zeroeth order solution would be promoted to a function of t , and would be corrected. In this simple case, the constant shifts $A \rightarrow 1 + \epsilon$, $\omega \rightarrow \omega - \epsilon\omega$ would suffice to cancel out the secular growth to linear order in ϵ .

The DRG has recently been reformulated by Galvez-Ghersi and Stein,¹⁵⁵ which they call the *numerical dynamical renormalization group*. This is because their approach allows for the renormalization of parameters for theories whose (background) solution may only be found numerically. We note that the application of the DRG formally requires the full solution to be described by a finite dimensional attractor manifold in parameter space. The Einstein (and Horndeski) equations of motion are partial differential equations, which formally have an infinite number of control parameters (for example, one needs to set $\phi, \partial_t \phi$ at each spatial point on the initial data slice). Because of this, it is not immediately obvious how the numerical DRG can be applied to generic solutions to these theories.

At least in the context of binary black hole mergers though, there is reason to believe the DRG could prove to be useful. From Post-Newtonian theory, it is known that the problem of binary black hole/neutron star inspiral can be very accurately described using a finite number of parameters; for a review see Ref. 156^j.

^jSurrogate modeling of gravitational waveforms also shows that gravitational waveforms for a

Thus one expects there is a finite-dimensional attractor manifold for the two-body problem in GR (and Horndeski gravity, and other modified theories of gravity). In principle then the numerical DRG should be able to control the secular divergences encountered in the modeling of gravitational waves from black holes/neutron inspiral for a variety of modified gravity theories, including potentially perturbative solutions to the Horndeski theories of gravity. In particular, the numerical DRG has been proposed to be applied directly to the gravitational waveforms computed from perturbative solutions to modified gravity theories.¹⁵⁵

8. Constructing exact initial data

As in GR, the equations of motion for the Horndeski theories form an overdetermined system of partial differential equations, and there are a set of constraint equations that must be satisfied on the initial data surface. In this section we will focus only on the exact constraint equations; the perturbative equations of motion (Sec. 4) reduce to those of the Einstein equations plus lower order terms, and thus can be solved using the same techniques already used in numerical relativity.¹⁵⁸

Let (M, g) be a smooth, 4-dimensional, globally hyperbolic spacetime. An initial data set is the set $(\Sigma, h_{ij}, K_{ij}, \phi, \partial_0 \phi)$, where Σ is a smooth 3-dimensional spacelike submanifold of M , h_{ij} and K_{ij} are the Riemannian metric and extrinsic curvature induced on Σ , and ϕ and $\partial_0 \phi$ are the scalar field and its first time derivative on Σ . The indices i, j run over the spatial tensor components induced on Σ . We denote the induced metric-compatible covariant derivative operator on the spatial hypersurface with D_i , and the induced Christoffel symbols and tensors with a ⁽³⁾ superscript.

The constraint equations can be cast into a generalization of the *Hamiltonian* and *momentum* constraints of GR. For a given Σ , we let n^μ be the unit timelike future-directed null vector orthogonal to Σ . We can then write the spacetime metric as

$$g_{\mu\nu} = -n_\mu n_\nu + h_{\mu\nu}. \quad (45)$$

The induced form of the metric $h_{\mu\nu}$ on Σ is h_{ij} . The covariant expression for the extrinsic curvature is

$$K_{\mu\nu} \equiv -h_\mu^{\alpha} h_\nu^{\beta} \nabla_\alpha n_\beta. \quad (46)$$

The generalized Hamiltonian and momentum constraints are defined to be

$$\mathcal{H} \equiv E_{\gamma\delta}^{(g)} n^\gamma n^\delta = 0, \quad (47)$$

$$M_\mu \equiv E_{\gamma\delta}^{(g)} n^\gamma h_\mu^\delta = 0. \quad (48)$$

There are two main challenges to constructing initial data:

variety of gravitational wave sources can be accurately described using a relatively small number of parameters.¹⁵⁷

- (1) Casting the constraint equations into a form that allows for a well-posed boundary value problem.
- (2) Relating the evolution variables $(g_{\mu\nu}, \phi)$ to physically meaningful quantities, to construct astrophysically realistic initial data.

A large number of techniques have been developed over the years to address these two problems in GR (for reviews, see Refs. 1, 2, 158). We review how some of these techniques can be extended to the problem of constructing constraint satisfying initial data for Horndeski gravity theories. In particular, in Sec. 8.2 we show that provided the Horndeski corrections are weakly coupled (for a review of this terminology see Sec. 3.2), the constraint equations can be shown to be elliptic under the conformal transverse-traceless decomposition, and in Sec. 8.3 we show how black hole “puncture” initial data has been extended to some Horndeski gravity theories.³⁴ There has been essentially no numerical work on constructing numerical solvers to the general constraint equations in Horndeski gravity.

8.1. The constraint equations: general properties

We pick ADM-like coordinates adapted to the spacelike hypersurface Σ , so that x^0 is the timelike coordinate:

$$g_{\mu\nu}dx^\mu dx^\nu = -N^2 (dx^0)^2 + h_{ij} (N^i dx^0 + dx^i) (N^j dx^0 + dx^j). \quad (49)$$

The unit orthogonal timelike vector is then $n_\alpha = (-N, 0, 0, 0)$. The lapse is N and the shift vector is N^i .

We first show that $\partial_0^2 \phi$ and $\partial_0^2 g_{\mu\nu}$ do not appear in the Horndeski constraint equations. From the constraint equations (47) (48) and tensor equations of motion (A.1), we see that the presence of second time derivatives comes from there being repeated 0 components in contractions with the generalized Kronecker delta tensor:

$$\begin{array}{ll} n_\alpha n^\beta \delta_{\beta\delta_1\delta_2}^{\alpha\gamma_1\gamma_2} & n_\alpha h_\mu^\beta \delta_{\beta\delta_1\delta_2}^{\alpha\gamma_1\gamma_2} \\ n_\alpha n^\beta \delta_{\beta\delta_1\delta_2\delta_3}^{\alpha\gamma_1\gamma_2\gamma_3} & n_\alpha h_\mu^\beta \delta_{\beta\delta_1\delta_2\delta_3}^{\alpha\gamma_1\gamma_2\gamma_3} \\ n_\alpha n^\beta \delta_{\beta\delta_1\delta_2\delta_3}^{\alpha\gamma_1\gamma_2\gamma_3} & n_\alpha h_\mu^\beta \delta_{\beta\delta_1\delta_2\delta_3}^{\alpha\gamma_1\gamma_2\gamma_3} \end{array}$$

From the contractions of the Riemann tensor (see Appendix E), in adapted coordinates we see that the only two time derivative terms that could act on the metric would come from the contraction $h_{\mu_1}{}^{\gamma_1} n^{\gamma_2} h^{\nu_1}{}_{\delta_1} n_{\delta_2} R_{\gamma_1\gamma_2}{}^{\delta_1\delta_2}$. From the contractions on $\nabla_\gamma \nabla^\delta \phi$ (see Appendix E), in adapted coordinates we see that the only two time derivative terms could come from contractions on two n^μ vectors (the derivatives D are purely spatial in the induced coordinates): $n^\mu n_\nu \nabla_\mu \nabla^\nu \phi$. Our task then is to show that there are no repeated n^μ vectors in the constraints with a raised/lowered index (for example there is no contraction like $n_\alpha n_{\gamma_1}$ in the constraints). By the antisymmetry of the Kronecker delta tensors we easily see this is the case. For example we have

$$n_\alpha h_\mu^\beta \delta_{\beta\delta_1\delta_2}^{\alpha\gamma_1\gamma_2} \times n_{\gamma_1} n^{\delta_1} h_{\gamma_2}^{\kappa_2} h_{\rho_2}^{\delta_2} \times \dots = 0. \quad (50)$$

Using a similar argument it is easy to show that there are no terms multiplying $\partial_0^2\phi$ or $\partial_0^2g_{\mu\nu}$ in the constraint equations in $4\partial ST$ (which we know must also be true as it is a special case of a Horndeski gravity theory).¹⁰⁷

We provide a more general argument that shows that there are no terms with second order time derivatives in the constraint equations for Horndeski gravity—which can be be straightforwardly generalized to scalar-tensor theories with multiple scalar fields,^{33, 125} vector tensor theories,^{159, 160} or more generally any tensor theory that has second order equations of motion that can be derived from an action—in Appendix D.

As a corollary of there being no second time derivatives in the constraint equations, we see that if we set

$$\phi|_{\Sigma} = \partial_0\phi|_{\Sigma} = 0, \quad (51)$$

then the constraint equations for Horndeski gravity reduce to those of vacuum GR. This follows because from Eq. (51) as it implies $\partial_{\mu}\phi = 0$ and $\partial_{\mu}\partial_i\phi = 0$, and we have already established there are no terms like $\partial_0^2\phi$ in the constraint equations. This result has also been shown to be true for $4\partial ST$ theory¹⁰⁷ (as before, we can alternatively note that these results hold for $4\partial ST$ theory as it is a Horndeski theory).

An additional corollary of the fact that there are no repeated time derivatives acting on the metric or scalar degrees of freedom is that the constraint equations can be formulated as a system of elliptic PDE when the Horndeski terms are weakly coupled. We sketch an argument that explicitly shows this to be true in a conformal transverse-traceless decomposition in Sec. 8.2.

8.2. Example: the elliptic character of the exact constraint equations under the conformal transverse-traceless (CTT) decomposition

Here we show in more detail how the constraints can be written as a set of elliptic equations for weakly coupled solutions by working with the conformal transverse-traceless (CTT) decomposition.¹⁶¹ We will only consider the principal part of the constraint equations, as it is the part that determines the character of the constraints as a set of PDE. Kovacs³⁴ has shown that for $4\partial ST$ gravity, for a weakly coupled solution under a CTT decomposition (and for a conformal thin sandwich decomposition) the constraints formed an elliptic set of PDE. Moreover, he showed that a unique solution exists to the elliptic boundary value problems on asymptotically Euclidean initial slices under similar conditions as in the case of General Relativity. In demonstrating the fundamental ellipticity of the constraint equations in the CTT formalism for the general constraint equations, this section demonstrates the plausibility of extending Kovacs proof to initial data for general Horndeski theories. We emphasize that other decompositions commonly used in numerical relativity could also likely lead to an elliptic set of constraint equations for the Horndeski gravity theories for weakly-coupled solutions.

The conformal (Lichnerowicz-York) decomposition is:

$$h_{ij} = \psi^4 \tilde{h}_{ij}, \quad (52)$$

$$K_{ij} = \frac{1}{\psi^2} \tilde{A}_{ij} + \frac{1}{3} \gamma_{ij} K, \quad (53)$$

where \tilde{A}_{ij} is traceless. Finally we decompose \tilde{A}_{ij} with a transverse decomposition

$$\tilde{A}_{ij} = (\tilde{L}W)_{ij} + \tilde{A}_{(TT)ij}, \quad (54)$$

$$(\tilde{L}W)_{ij} \equiv \tilde{D}_i W_j + \tilde{D}_j W_i - \frac{2}{3} \tilde{\gamma}_{ij} \tilde{D}_k W^k, \quad (55)$$

where \tilde{L} is the *longitudinal operator* (also called the *vector gradient*) and $\tilde{A}_{(TT)ij}$ is a transverse-traceless tensor: $\tilde{\gamma}^{ij} \tilde{A}_{(TT)ij} = \tilde{D}^i \tilde{A}_{(TT)ij} = 0$. As is the case in GR with a minimally coupled scalar field, the free degrees of freedom are

$$\tilde{\gamma}_{ij}, \quad K, \quad \tilde{A}_{(TT)ij}, \quad \phi, \quad \partial_0 \phi, \quad (56)$$

and the constraints will determine the degrees of freedom

$$\psi, \quad W_i. \quad (57)$$

We first study the Hamiltonian constraint:

$$\begin{aligned} \mathcal{H} = & -\frac{1}{4} (1 + \mathcal{G}_4 - 2X\partial_X \mathcal{G}_4 + X\partial_\phi \mathcal{G}_5) n_\alpha n^\beta \delta_{\beta\delta_1\delta_2}^{\alpha\gamma_1\gamma_2} R_{\gamma_1\gamma_2}^{\delta_1\delta_2} \\ & + \frac{1}{4} (\partial_X \mathcal{G}_4 - \partial_\phi \mathcal{G}_5) n_\alpha n^\beta \delta_{\beta\delta_1\delta_2\delta_3}^{\alpha\gamma_1\gamma_2\gamma_3} \nabla_{\gamma_1} \phi \nabla^{\delta_1} \phi R_{\gamma_2\gamma_3}^{\delta_2\delta_3} \\ & - \frac{1}{4} (X\partial_X \mathcal{G}_5) n_\alpha n^\beta \delta_{\beta\delta_1\delta_2\delta_3}^{\alpha\gamma_1\gamma_2\gamma_3} \nabla_{\gamma_1} \nabla^{\delta_1} \phi R_{\gamma_2\gamma_3}^{\delta_2\delta_3} \\ & + l.o.t. \end{aligned} \quad (58)$$

Given the antisymmetry of the Kronecker delta tensor, we see the only nonzero components of the Riemann tensor will come from contractions on $h_{\mu\nu}$. As $K_{\mu\nu}$ contains only first derivatives of the metric, we only focus on ${}^{(3)}R_{\mu_1\mu_2}{}^{\nu_1\nu_2}$: $\mathbb{P}[R_{\gamma_1\gamma_2}^{\delta_1\delta_2}] \rightarrow \mathbb{P}[{}^{(3)}R_{i_1i_2}{}^{j_1j_2}]$, and $\delta_{j\cdots}^i$ are the Kronecker delta tensors induced on the spatial surface Σ . Continuing to work in adapted coordinates, under the conformal decomposition we see that (see Appendix E)

$${}^{(3)}R_{i_1i_2}{}^{j_1j_2} = -8 \frac{1}{\psi^5} \delta_{[i_1}^{[j_1} \tilde{D}_{i_2]} \tilde{D}^{j_2]} \psi + l.o.t. \quad (59)$$

Plugging this in to Eq. (58), we see that the principal part of Hamiltonian constraint for the conformal factor is

$$\mathcal{H} = \tilde{\Delta} \psi + F(\partial_i \partial_j \psi) + l.o.t. \quad (60)$$

where the F contains terms that have second derivatives acting on ψ , but which are suppressed in the weakly-coupled limit. Provided then that the Horndeski terms are sufficiently weakly coupled (Eq. (16)), this is an elliptic equation for ψ as the

Laplacian $\tilde{\Delta} \equiv \tilde{D}_i \tilde{D}^i$ is elliptic. This follows as the principal symbol for the Laplacian is symmetric positive definite matrix, and for a sufficiently small symmetric perturbation, a symmetric positive definite matrix remains positive definite.

We next turn to the momentum constraint:

$$\begin{aligned} \mathcal{M}_\mu = & -\frac{1}{4} (1 + \mathcal{G}_4 - 2X\partial_X \mathcal{G}_4 + X\partial_\phi \mathcal{G}_5) n_\alpha h_\mu^\beta \delta_{\beta\delta_1\delta_2}^{\alpha\gamma_1\gamma_2} R_{\gamma_1\gamma_2}^{\delta_1\delta_2} \\ & + \frac{1}{4} (\partial_X \mathcal{G}_4 - \partial_\phi \mathcal{G}_5) n_\alpha h_\mu^\beta \delta_{\beta\delta_1\delta_2\delta_3}^{\alpha\gamma_1\gamma_2\gamma_3} \nabla_{\gamma_1} \phi \nabla^{\delta_1} \phi R_{\gamma_2\gamma_3}^{\delta_2\delta_3} \\ & - \frac{1}{4} (X\partial_X \mathcal{G}_5) n_\alpha h_\mu^\beta \delta_{\beta\delta_1\delta_2\delta_3}^{\alpha\gamma_1\gamma_2\gamma_3} \nabla_{\gamma_1} \nabla^{\delta_1} \phi R_{\gamma_2\gamma_3}^{\delta_2\delta_3} \\ & + l.o.t.. \end{aligned} \quad (61)$$

Given the antisymmetry of the Kronecker delta, the only nonzero contractions against the Riemann tensor will come from $h_{\mu_1}{}^{\gamma_1} h_{\mu_2}{}^{\gamma_2} h^{\nu_1}{}_{\delta_1} h_{\nu_2}{}^{\delta_2} R_{\gamma_1\gamma_2}{}^{\delta_1\delta_2}$, and $h_{\mu_1}{}^{\gamma_1} h_{\mu_2}{}^{\gamma_2} h^{\nu_1}{}_{\delta_1} n_{\delta_1} R_{\gamma_1\gamma_2}{}^{\delta_1\delta_2}$. From the latter contraction we see the principal part will come from ∇K terms; in adapted coordinates we have

$$D^{[j_2} K_{i_3]}^{j_1]} = \frac{1}{\psi^{10}} \tilde{D}^{[j_2} (\tilde{L}W)^{j_1]}_{i_3]} + l.o.t. \quad (62)$$

From $h_\nu^\mu n^\nu = 0$, we see that in adapted coordinates the momentum constraint is

$$\mathcal{M}^i = \left(\tilde{\Delta}_L W \right)^i + F^i (\partial_j \partial_k W^l, \partial_k \partial_k \psi) + l.o.t. \quad (63)$$

where F^i contains terms that have second derivatives acting on W^l and ψ , but which are suppressed in the weak-coupling limit. While there are now second derivatives of ψ in the momentum constraint, provided we work in the weak-coupling limit, the *system* of PDE formed by the Hamiltonian and momentum constraints remain fundamentally elliptic in character as the vector Laplacian $\left(\tilde{\Delta}_L W \right)^i \equiv \tilde{D}_j \left(\tilde{L}W \right)^{ij}$ is elliptic.

While we have shown that the constraint equations are fundamentally elliptic in Horndeski gravity, we reiterate that the well-posedness of asymptotically flat solutions to the constraint equations as a set of elliptic PDE has *not* yet been proven for general weakly-coupled Horndeski gravity theories. Such a proof has only recently been constructed by Kovacs³⁴ for $4\partial ST$ gravity, which contains a particular subset of the Horndeski theory terms. We expect though that a proof similar to his should follow for general Horndeski gravity theories, as his argument essentially rested on the fundamentally elliptic nature to the constraint PDE for weakly-coupled solutions, and the fact that nonlinear lower order terms generally do not control the solution properties of sufficiently regular asymptotically flat solutions.

8.3. Example: Bowen-York “puncture” initial data in $4\partial ST$ gravity

Kovacs has proposed a prescription to construct Bowen-York “black hole puncture” initial data³⁴ in $4\partial ST$ gravity^k This class of initial data has been widely used in GR as it transparently allows one to set the approximate mass, momentum, and spin of multiple black hole solutions.¹⁶²

Prescribing Bowen-York initial data in GR^{163,164} involves setting

$$\tilde{h}_{ij} = \delta_{ij}, \quad K = 0, \quad \tilde{A}_{(TT)}^{ij} = 0. \quad (64)$$

With the above conditions, in general relativity the momentum constraint equation can be solved with

$$W^i = -\frac{1}{4r} (7P^i + P^j \hat{x}_j \hat{x}^i) - \frac{1}{r^2} \epsilon^{ijk} S_j \hat{x}_k, \quad (65)$$

where x^i are the Euclidean coordinates in \mathbb{R}^3 , $r = \sqrt{\delta_{ij} x^i x^j}$ is the Euclidean distance from the puncture, \hat{x}^i/r is the unit Euclidean vector, and ϵ^{ijk} is the Levi-Cevita symbol. The free initial data are the vectors P^i, S^i . The vector P^i corresponds to the total ADM linear momentum of the spacetime, and S^i is the total ADM angular momentum of the spacetime,¹⁶³ that is with these choices we have

$$P_{ADM}^i \equiv \frac{1}{8\pi} \lim_{r \rightarrow \infty} \int_{S_2} dA (K^{ij} - K h^{ij}) \hat{x}_j = P^i, \quad (66a)$$

$$S_{ADM}^i \equiv \frac{1}{8\pi} \lim_{r \rightarrow \infty} \int_{S_2} dA (K_{jk} - K h_{jk}) \epsilon^{ijl} x_l \hat{x}^k = S^i. \quad (66b)$$

While these are global quantities, it turns out they are typically close to the quasi-local definitions of the black hole linear and angular momentum. The remainder of the momentum is carried in “junk radiation”, the amount of which is typically dependent on the initial black hole spin. As the momentum constraint is linear in W^i , this initial data can be superposed for a collections of black holes

$$W^i = - \sum_n \left(\frac{1}{4r_{(n)}} \left(7 \left(P^{(n)} \right)^i + \left(P^{(n)} \right)^j \hat{x}_j \hat{x}^i \right) + \frac{1}{r_{(n)}^2} \epsilon^{ijk} \left(S^{(n)} \right)_j \hat{x}_k \right), \quad (67)$$

where $r_{(n)} \equiv |\mathbf{x} - \mathbf{c}_{(n)}|$, the Euclidean distance from the n^{th} puncture ($\mathbf{c}_{(n)}$ are at the black hole puncture locations). With puncture initial data, we still need to solve the Hamiltonian constraint numerically, which forms an elliptic equation for ψ . This can be solved more easily by making the following field redefinition¹⁶⁴

$$\psi = 1 + \frac{1}{\mu} + u, \quad \frac{1}{\mu} \equiv \sum_n \frac{m_{(n)}}{2r_{(n)}}, \quad (68)$$

^kWe restrict ourselves to $4\partial ST$ gravity as—at least as of the publication of this review—there is no general proposal for black hole puncture initial data for general Horndeski gravity theories.

That is, we analytically remove the “singular” term from the conformal factor. This renders the solution ψ to be regular (more precisely, C^2 ; see 164) throughout \mathbb{R}^3 for asymptotically flat boundary conditions.

Kovacs³⁴ has generalized this initial data for 4 ∂ ST gravity. While this only contains a particular subset of Horndeski gravity, it does contain the term that causes scalar “hairy” black holes (namely, the Gauss-Bonnet coupling $\beta(\phi)\mathcal{G}$), so it is perhaps the most interesting Horndeski theory to study in the context of binary black hole systems. His construction relies on the linearity of the momentum constraint for the theory when it is written in terms of the canonical conjugate momentum for the tensor and scalar degree of freedom^{134,165}

$$\pi^{ij} \equiv \frac{\delta\mathcal{L}}{\delta(\partial_0 h^{ij})}, \quad \pi_\phi \equiv \frac{\delta\mathcal{L}}{\delta(\partial_0 \phi)}. \quad (69)$$

Kovacs’ prescription for puncture initial data is to then decompose π^{ij} and π_ϕ in the following way:

$$\tilde{\pi}_{ij} \equiv \psi^2 \left(\frac{1}{\sqrt{h}} \pi_{ij} - \frac{1}{3} h^{kl} \pi_{kl} h_{ij} \right), \quad \tilde{\pi}_\phi \equiv \psi^6 \frac{\pi_\phi}{\sqrt{h}}. \quad (70)$$

Then the trace is set to zero, and the tracefree part is set to the same functional form as the tracefree part of the extrinsic curvature is in GR:

$$\tilde{h}_{ij} = \delta_{ij}, \quad (71a)$$

$$\tilde{\pi}_\phi = 0, \quad (71b)$$

$$\tilde{\pi}_{ij} = \partial_i W_j + \partial_j W_i - \frac{2}{3} \delta_{ij} \partial_k W^k, \quad (71c)$$

$$W^i = - \sum_n \left(\frac{1}{4r_{(n)}} \left(7 \left(P^{(n)} \right)^i + \left(P^{(n)} \right)^j \hat{x}_j \hat{x}^i \right) + \frac{1}{r_{(n)}^2} \epsilon^{ijk} \left(S^{(n)} \right)_j \hat{x}_k \right). \quad (71d)$$

As the canonical momentum reduces to the extrinsic curvature in the asymptotically flat limit ($r \rightarrow \infty$), it is straightforward to show that the spacetime linear and angular momentum are set by the total P^i and S^i (see Eq. (66)).³⁴ We have also defined a traceless and conformally rescaled conjugate momentum. In this setup, the fields $\phi, \partial_0 \phi$ can be freely specified so long as they satisfy $\tilde{\pi}_\phi = 0$. This initial data satisfies the momentum constraint in 4 ∂ ST gravity, and in the weak-coupling limit the conformal factor ψ obeys an elliptic equation of motion (the Hamiltonian constraint).

¹We note that while the relation between the canonical momenta π^{ij}, π_ϕ and $K_{ij}, \partial_t \phi$ for 4 ∂ ST gravity is nonlinear,¹⁶⁵ for weakly-coupled solutions it is possible to relate the two by iteratively solving the relations Eq. (69).³⁴

9. Evolution of compact objects in Horndeski gravity theories: a brief survey of numerical work

9.1. *Bergmann–Wagoner scalar-tensor theories*

First we survey the numerical evolution of “scalar-tensor” gravity theories (see also Sec. 5.3). Most numerical work for these theories has been in the Einstein frame, where there is no scalar-tensor coupling in the principal part of the equations of motion. In that frame, from a numerical standpoint evolving the equations of motion for scalar-tensor theories is no more difficult than evolving the equations of motion for minimally a coupled scalar field. Due to the no-hair theorems for black holes in these theories,^{54,166} numerical work on this theory has focused on the evolution of (binary) neutron stars, which can exhibit interesting solutions such as *spontaneous scalarization*.⁵⁶ Some work on black holes in these theories has been performed in spherical symmetry as well.^{167,168} In particular, much of the numerical work on scalar-tensor theories has focused on stellar collapse of a spherically symmetric scalarized star to a black hole, as in the process of forming a black hole the star must shed a large amount of scalar hair, which could be potentially observable through measurement of a scalar polarization mode in gravitational waves.^{169–178} Other work in spherical symmetry has been done on scalarized stars,¹⁷⁹ including studies of potential *screening* effects^{80,100,180,181} of these theories.¹⁸² Relatively little work on full 3 + 1 collisions of scalarized stars has been done for scalar-tensor gravity theories.

9.2. *Quadratic Horndeski gravity*

The quadratic Horndeski theories have been used to construct models of dark energy/inflation^{91,92} that have not been observationally ruled out.^{24,183,184} Moreover solutions to variants of the theory can exhibit a screening mechanism⁸⁰ called *k-mouflage*,¹⁸⁵ whereby the spacetime geometry around a scalarized star can closely resemble the vacuum exterior of an unscalarized star. Numerical work on the quadratic gravity theories has focused mostly on investigating the well-posedness of these theories in the strong field, dynamical regime.^{27,113,135} In particular, there has been work on investigating the formation of shocks and sonic lines in these theories, and the dynamics of the theory during the onset of k-mouflage,^{103,104,182} which can move the solution to the strongly-coupled regime. Asymptotically flat black holes cannot support stable scalar hair (outside of super-radiance),¹⁸⁶ so much of the attention has been focused on (neutron) star solutions.

More recently, Bezares et. al.⁹⁴ have performed full 3 + 1 evolution of binary neutron star mergers in a variant of quadratic gravity that was predicted to lead to screening. To deal with the potential formation of shocks, the authors made use of high resolution shock capturing methods. In that reference, the authors found certain functional forms of the theory that appears to allow for evolution without the formation of elliptic regions, even in the strongly coupled regime.

9.3. Cubic Horndeski gravity

Figueras and França^{40,97} have recently performed the first fully-nonlinear simulations of dynamical black hole spacetimes in a cubic Horndeski gravity theory. In both works, they considered couplings of the form $\mathcal{G}_2 = g_2 X^2$ and $\mathcal{G}_3 = g_3 X$, where g_2 and g_3 are constants, and either $V = 0$ ⁴⁰ or $V = \frac{1}{2}m^2\phi^2$.⁹⁷ To evolve the equations of motion in well-posed fashion, the authors rewrote the equations of motion as described by Kovacs,²⁸ and then made use of the CCZ4 formulation^{95,96} (see also Sec. 5.2).

From spherical collapse simulations Figueras and França found that the equations of motion for cubic Horndeski gravity can dynamically form a sonic line and elliptic region outside of a black hole horizon.⁴⁰ This loss of hyperbolicity is located in the scalar sector of the theory. Despite the loss of hyperbolicity in the strongly coupled regime, the theory did remain hyperbolic in regions where the solution remained safely in the weakly-coupled regime. As the authors used CCZ4 puncture-type evolution,¹⁸⁷ to avoid hyperbolicity issues in the interior of the black hole they smoothly turned off the coefficients g_2 and g_3 inside the apparent horizon. In particular, they multiplied the coefficients by a sigmoid function

$$g_i \rightarrow g_i \times \frac{1}{1 + e^{-\frac{2}{w}((x/\bar{x})-1)}}, \quad (72)$$

where x is a distance measure from the “center” of the black hole to the apparent horizon, and \bar{x}, w are pre-set constants^m. As a measure of the distance inside the black hole, Figueras and França used the value of the conformal factor χ in the CCZ4 formulation, the level sets of which have been empirically shown to closely follow the apparent horizons of black hole and black strings^{188,189} (for example, for Schwarzschild black holes in moving puncture gauge, within the CCZ4 formulation the black hole apparent horizon settles to around $\chi \sim 0.25$ ⁴⁰).

Following this work, Figueras and França considered binary black hole collisions for the same kinds of theories.⁹⁷ In this work, initial data was set by super-imposing two boosted spherically symmetric solutions of lumps of scalar field ϕ . While this does not exactly solve the constraints, provided the black holes are far enough apart, it provides a reasonably close solution to the full equations of motion. The two lumps of scalar field quickly collapsed to forming black holes with some leftover scalar field energy outside of the black holes. While black holes cannot support scalar field hair for the class of Horndeski theories they consider,^{190,191} the initial data the authors choose allowed for some residual scalar field during the inspiral, which they showed lead to some dephasing of eccentric black hole binaries as compared to GR.⁹⁷

^mWhile the sigmoid will not be exactly one for all $x < \infty$, it rapidly transitions to values very close to 1 for x outside of a narrow “transition region” whose location and width are determined by \bar{x} and w , respectively.

9.4. *4 ∂ ST gravity (alias Einstein scalar Gauss-Bonnet (ESGB) gravity)*

Einstein scalar Gauss-Bonnet (ESGB) gravity (See Eq. (11)) has received much attention recently as variants of ESGB gravity allow for scalar “hairy” black holes.^{21,22,46} This can be seen by considering the scalar field equation of motion (Eq. (A.4))

$$\begin{aligned} E^{(\phi)} = & \square\phi - V' \\ & + 3\alpha X\square\phi - 2\alpha\nabla^\alpha\phi\nabla^\beta\phi\nabla_\alpha\nabla_\beta\phi - 3\alpha'X^2 \\ & + \beta'\mathcal{R}_{GB}. \end{aligned} \quad (73)$$

For Schwarzschild and Kerr black holes, $\mathcal{R}_{GB} \neq 0$, thus even if $\phi = \partial_0\phi = 0$ at $t = 0$, provided $\beta'(0) \neq 0$, the scalar field sees a nonzero “source” term, which causes it to grow about the black hole. For example, in “shift-symmetric scalar Gauss-Bonnet gravity” $V = \alpha = 0$ and $\beta = \lambda\phi$, where λ is a constant. This theory has scalar-hairy black holes, while neutron stars in the theory remain relatively less hairy, so binary black hole systems may provide the strongest constraints on these theories.¹⁹² This theory has been extensively studied, using the order reduction approach,^{81–83, 193, 194} in the static limit,^{46, 195} and restricted to spherically symmetric spacetimes.^{39, 75} The first fully nonlinear simulations of this theory of binary black hole spacetimes were completed using the MGH formulation, with vacuum GR black hole initial data.¹⁰⁷

Even if $\beta'(0) = 0$, GR black holes can still be unstable to *spontaneous black hole scalarization*^{48–50, 196–199} (which is analogous to spontaneous scalarization for neutron stars in scalar-tensor gravity⁵⁶—see also Sec. 9.1). This can be seen by expanding Eq. (73) in powers of ϕ (assuming $\phi \ll 1$):

$$0 = \square\phi - (V'' - \beta''\mathcal{R}_{GB})\phi + \mathcal{O}(\phi^2). \quad (74)$$

We see that $\beta''\mathcal{R}_{GB}$ can act as an “effective” mass, that could lead to a tachyonic instability depending on the sign of that term. There have been several recent numerical simulations of binary black hole systems that exhibit spontaneous black hole scalarization (and de-scalarization), using order reduction methods^{200, 201}ⁿ. Fully nonlinear simulations of binary black holes in a variant of this theory that exhibits black hole scalarization has only been performed for head-on collisions.⁴¹

Evolving exact solutions through the merger for scalar-hairy black holes in this theory (that is when $\beta \neq 0$) has proven to be challenging, as during the merger phase, spacetime curvature gradients can grow large, which could trigger the formation of new elliptic regions. Provided these new elliptic regions remain inside the event horizon of the final black hole a given theory can remain theoretically viable, but excising these regions using black hole excision can be challenging before an apparent horizon for the final black hole has been found.

ⁿWe note that one potential limitation of the perturbative approach for theories that are dynamically unstable to scalarization is that nonlinear effects are generally needed to *saturate* the instability.

The study of binary black hole systems for other values of scalar field potential V and coupling α remains relatively less studied, at least together with nontrivial values of β .

10. Final remarks

We have reviewed the status of numerically constructing black hole/neutron star solutions in Horndeski theories of gravity. We discussed exact and perturbative methods that give well-posed formulations of the evolution and constraint equations, at least for so-called *weakly-coupled* solutions. Both the exact and perturbative approaches introduce new difficulties not encountered in numerical solutions of the Einstein equations. Exact solutions may suffer from the formation of shocks or a loss of hyperbolicity, while perturbative solutions must contend with the secular growth of errors in time. Many basic questions about the Horndeski theories remain unanswered, especially in the context of binary black hole and neutron star mergers, and much work remains to properly understand how to (numerically) solve and interpret the equations of motion for these theories. Nevertheless, there are several promising ways to extend numerical relativity methods to construct strong gravity, weakly coupled solutions to the Horndeski gravity theories.

Acknowledgments

I thank Aron Kovacs, Frans Pretorius, Harvey Reall, Leo Stein, Maxence Corman, Nicolas Yunes, Ulrich Sperhake, and William East for helpful discussions, and thank Abhishek Hegde, Aron Kovacs, Tomas Galvez-Ghersi, Maxence Corman, Tiago Fran  a, and William East for helpful comments on an earlier draft of this article. While writing this article I was supported by STFC Research Grant No. ST/V005669/1.

Appendix A. Equations of motion for Horndeski gravity

Varying (1) with respect to the metric and scalar fields, we obtain the tensor and scalar equations of motion, respectively. These were first derived by Horndeski.¹⁷ We have checked the equations in Papallo⁷³ (See also Tanahashi and Ohashi¹²⁵ for the “shift-symmetric” Horndeski equations of motion, which are when the \mathcal{G}_i only depend on derivatives of ϕ) using the `xTensor`^{202–204} package for `Mathematica`. Due to our different normalization for R , there is a factor of 2 difference between the tensor equations of motion presented here and those presented in Papallo.⁷³ Our `Mathematica` notebook, along with other code used to generate some of the plots

used in this article, can be accessed online.²⁰⁵

$$\begin{aligned}
\left(E^{(g)}\right)^\alpha_\beta = & \\
& -\frac{1}{4}(1+2\mathcal{G}_4-4X\partial_X\mathcal{G}_4+2X\partial_\phi\mathcal{G}_5)\delta_{\beta\delta_1\delta_2}^{\alpha\gamma_1\gamma_2}R_{\gamma_1\gamma_2}^{\delta_1\delta_2} \\
& +\frac{1}{2}(\partial_X\mathcal{G}_4-\partial_\phi\mathcal{G}_5)\delta_{\beta\delta_1\delta_2\delta_3}^{\alpha\gamma_1\gamma_2\gamma_3}\nabla_{\gamma_1}\phi\nabla^{\delta_1}\phi R_{\gamma_2\gamma_3}^{\delta_2\delta_3} \\
& -\frac{1}{2}(X\partial_X\mathcal{G}_5)\delta_{\beta\delta_1\delta_2\delta_3}^{\alpha\gamma_1\gamma_2\gamma_3}\nabla_{\gamma_1}\nabla^{\delta_1}\phi R_{\gamma_2\gamma_3}^{\delta_2\delta_3} \\
& -(-V+X+\mathcal{G}_2+2X\partial_\phi\mathcal{G}_3+4X\partial_\phi^2\mathcal{G}_4)\delta_\beta^\alpha \\
& -(1+\partial_X\mathcal{G}_2+2\partial_\phi\mathcal{G}_3+2\partial_\phi^2\mathcal{G}_4)\nabla_\beta\phi\nabla^\alpha\phi \\
& +2(X\partial_X\mathcal{G}_3+\partial_\phi\mathcal{G}_4+2X\partial_X\partial_\phi\mathcal{G}_4)\delta_{\beta\delta}^{\alpha\gamma}\nabla_\gamma\nabla^\delta\phi \\
& +(\partial_X\mathcal{G}_3+4\partial_X\partial_\phi\mathcal{G}_4-\partial_\phi^2\mathcal{G}_5)\delta_{\beta\delta_1\delta_2}^{\alpha\gamma_1\gamma_2}\nabla_{\gamma_1}\phi\nabla^{\delta_1}\phi\nabla_{\gamma_2}\nabla^{\delta_2}\phi \\
& +(\partial_X\mathcal{G}_4+2X\partial_X^2\mathcal{G}_4-\partial_\phi\mathcal{G}_5-X\partial_X\partial_\phi\mathcal{G}_5)\delta_{\beta\delta_1\delta_2}^{\alpha\gamma_1\gamma_2}\nabla_{\gamma_1}\nabla^{\delta_1}\phi\nabla_{\gamma_2}\nabla^{\delta_2}\phi \\
& +(\partial_X^2\mathcal{G}_4-\partial_X\partial_\phi\mathcal{G}_5)\delta_{\beta\delta_1\delta_2\delta_3}^{\alpha\gamma_1\gamma_2\gamma_3}\nabla_{\gamma_1}\nabla^{\delta_1}\phi\nabla_{\gamma_2}\nabla^{\delta_2}\phi\nabla_{\gamma_3}\nabla^{\delta_3}\phi \\
& -\frac{1}{3}(\partial_X\mathcal{G}_5+X\partial_X^2\mathcal{G}_5)\delta_{\beta\delta_1\delta_2\delta_3}^{\alpha\gamma_1\gamma_2\gamma_3}\nabla_{\gamma_1}\nabla^{\delta_1}\phi\nabla_{\gamma_2}\nabla^{\delta_2}\phi\nabla_{\gamma_3}\nabla^{\delta_3}\phi, \tag{A.1}
\end{aligned}$$

$$\begin{aligned}
E^{(\phi)} = & \\
& -(1+\partial_X\mathcal{G}_2+2X\partial_X^2\mathcal{G}_2+2\partial_\phi\mathcal{G}_3+2X\partial_X\partial_\phi\mathcal{G}_3)\square\phi \\
& -(\partial_X^2\mathcal{G}_2+2\partial_X\partial_\phi\mathcal{G}_3+2\partial_X\partial_\phi^2\mathcal{G}_4)\delta_{\delta_1\delta_2}^{\gamma_1\gamma_2}\nabla_{\gamma_1}\phi\nabla^{\delta_1}\phi\nabla_{\gamma_2}\nabla^{\delta_2}\phi \\
& -(\partial_X\mathcal{G}_3+X\partial_X^2\mathcal{G}_3+2X\partial_X^2\partial_\phi\mathcal{G}_4+3\partial_X\partial_\phi\mathcal{G}_4)\delta_{\delta_1\delta_2}^{\gamma_1\gamma_2}\nabla_{\gamma_1}\nabla^{\delta_1}\phi\nabla_{\gamma_2}\nabla^{\delta_2}\phi \\
& -\frac{1}{4}(\partial_X\mathcal{G}_3+4\partial_X\partial_\phi\mathcal{G}_4-\partial_\phi^2\mathcal{G}_5)\delta_{\delta_1\delta_2\delta_3}^{\gamma_1\gamma_2\gamma_3}\nabla_{\gamma_1}\phi\nabla^{\delta_1}\phi R_{\gamma_1\gamma_2}^{\delta_1\delta_2} \\
& -(X\partial_X\mathcal{G}_3+\partial_\phi\mathcal{G}_4+2X\partial_X\partial_\phi\mathcal{G}_4)R \\
& -\frac{1}{2}(\partial_X^2\mathcal{G}_3+4\partial_X^2\partial_\phi\mathcal{G}_4-\partial_X\partial_\phi^2\mathcal{G}_5)\delta_{\delta_1\delta_2\delta_3}^{\gamma_1\gamma_2\gamma_3}\nabla_{\gamma_1}\nabla^{\delta_1}\phi\nabla_{\gamma_2}\nabla^{\delta_2}\phi\nabla_{\gamma_3}\nabla^{\delta_3}\phi \\
& -\frac{1}{2}(\partial_X\mathcal{G}_4+2X\partial_X^2\mathcal{G}_4-\partial_\phi\mathcal{G}_5-X\partial_X\partial_\phi\mathcal{G}_5)\delta_{\delta_1\delta_2\delta_3}^{\gamma_1\gamma_2\gamma_3}\nabla_{\gamma_1}\nabla^{\delta_1}\phi R_{\gamma_2\gamma_3}^{\delta_2\delta_3} \\
& -\frac{1}{2}(\partial_X^2\mathcal{G}_4-\partial_X\partial_\phi\mathcal{G}_5)\delta_{\delta_1\delta_2\delta_3\delta_4}^{\gamma_1\gamma_2\gamma_3\gamma_4}\nabla_{\gamma_1}\nabla^{\delta_1}\phi\nabla_{\gamma_2}\nabla^{\delta_2}\phi R_{\gamma_3\gamma_4}^{\delta_3\delta_4} \\
& -\frac{1}{3}(3\partial_X^2\mathcal{G}_4+2X\partial_X^3\mathcal{G}_4-2\partial_X\partial_\phi\mathcal{G}_5-X\partial_X^2\partial_\phi\mathcal{G}_5)\delta_{\delta_1\delta_2\delta_3}^{\gamma_1\gamma_2\gamma_3}\nabla_{\gamma_1}\nabla^{\delta_1}\phi\nabla_{\gamma_2}\nabla^{\delta_2}\phi\nabla_{\gamma_3}\nabla^{\delta_3}\phi \\
& -\frac{1}{3}(\partial_X^3\mathcal{G}_4-\partial_X^2\partial_\phi\mathcal{G}_5)\delta_{\delta_1\delta_2\delta_3\delta_4}^{\gamma_1\gamma_2\gamma_3\gamma_4}\nabla_{\gamma_1}\nabla^{\delta_1}\phi\nabla_{\gamma_2}\nabla^{\delta_2}\phi\nabla_{\gamma_3}\nabla^{\delta_3}\phi\nabla_{\gamma_4}\nabla^{\delta_4}\phi \\
& +\frac{1}{12}(2\partial_X^2\mathcal{G}_5+X\partial_X^3\mathcal{G}_5)\delta_{\delta_1\delta_2\delta_3\delta_4}^{\gamma_1\gamma_2\gamma_3\gamma_4}\nabla_{\gamma_1}\nabla^{\delta_1}\phi\nabla_{\gamma_2}\nabla^{\delta_2}\phi\nabla_{\gamma_3}\nabla^{\delta_3}\phi\nabla_{\gamma_4}\nabla^{\delta_4}\phi \\
& +\frac{1}{4}(\partial_X\mathcal{G}_5+X\partial_X^2\mathcal{G}_5)\delta_{\delta_1\delta_2\delta_3\delta_4}^{\gamma_1\gamma_2\gamma_3\gamma_4}\nabla_{\gamma_1}\nabla^{\delta_1}\phi\nabla_{\gamma_2}\nabla^{\delta_2}\phi R_{\gamma_3\gamma_4}^{\delta_3\delta_4} \\
& +\frac{1}{16}(X\partial_X\mathcal{G}_5)\delta_{\delta_1\delta_2\delta_3\delta_4}^{\gamma_1\gamma_2\gamma_3\gamma_4}R_{\gamma_1\gamma_2}^{\delta_1\delta_2}R_{\gamma_3\gamma_4}^{\delta_3\delta_4} \\
& +2X(\partial_\phi^2\mathcal{G}_3+\partial_X\partial_\phi\mathcal{G}_2)X-\partial_\phi\mathcal{G}_2+\partial_\phi V. \tag{A.2}
\end{aligned}$$

While 4 ∂ST gravity can be written in terms of a Horndeski theory, for completeness we list its equations of motion here as well

$$\begin{aligned} E^\alpha_\beta &= R^\alpha_\beta - \frac{1}{2}\delta^\alpha_\beta R - \nabla^\alpha\phi\nabla_\beta\phi + (-X + V)\delta^\alpha_\beta \\ &\quad - 2\alpha X\nabla^\alpha\phi\nabla_\beta\phi - \alpha X^2\delta^\alpha_\beta \\ &\quad + 2\delta^{\mu\rho\gamma\alpha}_{\nu\sigma\delta\beta}R^{\nu\sigma}_{\mu\rho}\nabla^\delta\nabla_\gamma\beta, \end{aligned} \quad (\text{A.3})$$

$$\begin{aligned} E^{(\phi)} &= \square\phi - V' \\ &\quad + 3\alpha X\square\phi - 2\alpha\nabla^\alpha\phi\nabla^\beta\phi\nabla_\alpha\nabla_\beta\phi - 3\alpha' X^2 \\ &\quad + \beta'\mathcal{R}_{GB}. \end{aligned} \quad (\text{A.4})$$

Appendix B. Hyperbolicity and well-posedness of evolution (hyperbolic) partial differential equations

For completeness, here we review some general concepts about the initial value problem for hyperbolic systems of partial differential equations (PDEs), several different notions of hyperbolicity, and state several theorems that relate hyperbolicity and the well-posedness of the initial value problem. There are many reviews on this subject, some of which are specialized for application in mathematical/numerical relativity,^{62,63,142,206,207} so we will only briefly outline the main ideas.

We consider systems of first order PDEs that take the form

$$A_J^I(x^\alpha, v^K, \partial_i v) \partial_0 v^J + B^I(x^\alpha, v^K, \partial_i v^L) = 0, \quad (\text{B.1})$$

where $I, J, \dots = 1, \dots, N$ index the N equations of motion and dynamical fields v^J , $i, j, \dots = 1, \dots, n$ index the n spatial coordinates, and $\alpha, \beta, \dots = 0, \dots, n$ index the $n+1$ spacetime coordinates. We note that through field redefinitions, we can write systems of second order equations that are linear in $\partial_0^2 v^J$

$$\begin{aligned} Y_J^I(x^\alpha, v^K, \partial_0 v^L, \partial_i v^M, \partial_i \partial_0 v^N, \partial_i \partial_j v^P) \partial_0^2 v^J \\ + Z^I(x^\alpha, v^K, \partial_0 v^L, \partial_i v^M, \partial_i \partial_0 v^N, \partial_i \partial_j v^P) = 0, \end{aligned} \quad (\text{B.2})$$

in the form (B.1).^{30,62,63} The equations of motion for Einstein gravity, Horndeski gravity, Lovelock gravity, and Einstein-Maxwell theory all can be written in the form of (B.2).^{30,42,160}

Provided A_J^I is invertible, we can rewrite Eq. (B.1) as

$$\partial_0 v^I + C^I(x^\alpha, v^J, \partial_i v^K) = 0. \quad (\text{B.3})$$

where

$$C_J^I \equiv (A^{-1})_J^K B^K. \quad (\text{B.4})$$

For the remainder of this section we will assume this to be the case.

Appendix B.1. Well-posedness

We say that the system (B.1) has a *well-posed initial value problem (well posed IVP)* if there exist constants A and α such that for all smooth enough initial data f^I , the solution remains uniformly bounded by an exponential

$$|v^I|(t) \leq Ae^{\alpha t} |f^I|. \quad (\text{B.5})$$

Here we use the L^2 norm

$$|v^I|(t) \equiv \sqrt{\int_{\mathbb{R}^3} d^3x (v_I)^\dagger v^I}. \quad (\text{B.6})$$

This condition guarantees that the solution depends continuously on the initial data.

Appendix B.2. Characteristics and notions of hyperbolicity

The *principal symbol* is defined to be

$$\mathcal{P}_J^I(\xi_\alpha) \equiv \delta_J^I \xi_0 + \left(\frac{\delta C^I}{\delta(\partial_i v^J)} \right) \xi_i, \quad (\text{B.7})$$

where ξ_α is an n dimensional unit covector, and ξ_i is a unit spatial covector. A *characteristic surface* $\Sigma \subset M$ is spanned by co-vectors that satisfy the *characteristic equation*

$$\det(\mathcal{P}_J^I(\xi_\alpha)) = 0. \quad (\text{B.8})$$

Replacing ξ_a with ∂_a , one obtains from (B.8) the *eikonal equation* for the characteristic surface.⁶⁴ Finally, for the n^{th} real solution to the characteristic equation, we define the *characteristic velocity* to be

$$c_i^{(n)} \equiv -\frac{\xi_i^{(n)}}{\xi_0^{(n)}}. \quad (\text{B.9})$$

We define the *characteristic speed* to be the 2-norm of the characteristic velocity, $c \equiv \sqrt{\sum_i |c_i|_2^2}$.

In order to determine the *hyperbolicity* of the system (B.3), we linearize the equations about a background solution v_0^I , about a given point $x^\alpha = x_0^\alpha$:

$$v^I \rightarrow v_0^I + \epsilon u^I, \quad (\text{B.10})$$

where $\epsilon \ll 1$. We then have a linear PDE for u^I :

$$\left(\delta_J^I \partial_0 + [F_J^I]^i \partial_i \right) u^J + G_J^I u^J = 0, \quad (\text{B.11})$$

where

$$[F_J^I]^i \equiv \left. \frac{\delta C^I}{\delta(\partial_i v^J)} \right|_{v^I=v_0^I}, \quad G_J^I \equiv \left. \frac{\delta C^I}{\delta v^J} \right|_{v^I=v_0^I}. \quad (\text{B.12})$$

We now define different notions of hyperbolicity. Provided A_J^I is invertible, at $x^\alpha = x_0^\alpha$ and $v^I = v_0^I$ the system (B.1) is *weakly hyperbolic* if all the eigenvalues of $[F_J^I]^i \xi_i$ are real for all unit ξ_i . The system is *strongly hyperbolic* if $[F_J^I]^i \xi$ has a complete set of eigenvectors that have real eigenvalues, and that the matrix whose columns are the eigenvectors, $T_J^I(\xi_i)$, satisfies

$$|T_J^I(\xi_i)| + \left| (T^{-1})_J^I(\xi_i) \right| \leq \Lambda, \quad (\text{B.13})$$

where Λ is a constant independent of ξ_i . Here $|\cdots|$ is a matrix norm. If the eigenvectors depend continuously on ξ_i , then (B.13) is satisfied since ξ_i is varied over a compact set (recall we impose that ξ_i has unit norm). Sometimes the eigenvectors are called “eigenfields”.¹

Before continuing, we mention another (equivalent) definition of strong hyperbolicity that is commonly used (see 207, 42, 30, 35). The system (B.1) is strongly hyperbolic if there is a smooth, positive definite $N \times N$ Hermitian matrix $H_J^I(\xi_i)$ —the *(Kreiss-)symmetrizer*—and a positive constant Λ such that for all ξ_i

$$H_K^I(\xi_j) [F_J^K]^i \xi_i = \left([F_K^I]^i \xi_i \right)^\dagger H_J^K(\xi_j), \quad (\text{B.14})$$

and

$$\frac{1}{\Lambda} |\delta_J^I| \leq |H_J^I(\xi_j)| \leq \Lambda |\delta_J^I|. \quad (\text{B.15})$$

This definition is equivalent to the earlier definition as one can show that

$$H_J^I \equiv \left((V^{-1})^\dagger \right)_K^I (V^{-1})_J^K, \quad (\text{B.16})$$

where the columns of V_J^I are the eigenvectors to $[F_J^I]^i \xi_i$, is a symmetrizer.

We can relate strong hyperbolicity to well-posedness of the initial value problem for systems of the form (B.3) with the following theorem (for a proof, see Chapter 5 of Taylor;²⁰⁸ note that in that reference the author calls strong hyperbolicity *symmetrizable hyperbolicity*):

Theorem For strongly hyperbolic systems (B.3), the Cauchy problem with initial data $v^I(0, \xi) = f^I(\xi)$ is well-posed in Sobolev spaces \mathbb{H}^s with $s > s_0$ for some constant s_0 . That is to say, there exists a unique local solution $v^I \in C([0, T), \mathbb{R}^d)$ with $T > 0$ depending on the \mathbb{H}^s -norm of the initial data.

The Sobolev space \mathbb{H}^s is the space of functions that have a finite Sobolev norm

$$|v|_{2,s} \equiv \sqrt{\sum_{k=0}^s \int_{\mathbb{R}^3} d^3x |\partial_i^K v|^2}, \quad (\text{B.17})$$

where ∂_i^K schematically stands for the sum over all spatial derivatives of order k .

In order words, for sufficiently regular initial data, a strongly hyperbolic system of PDE has a well-posed IVP. In physics applications the initial data is often very smooth (unless the initial data has “shocks”), so we will not discuss issues about optimal regularity of initial data.

Appendix B.3. Physical interpretation of characteristics

We end by briefly reviewing a “physical” interpretation for characteristic surfaces. First we rewrite (B.11) as

$$\mathcal{P}_J^I(\partial_\alpha) u^J + G_J^I u^J = 0. \quad (\text{B.18})$$

We next consider high frequency plane wave-like solutions:

$$u^I(x^\alpha) = \tilde{u}^I(x^i) e^{-ik_\alpha x^\alpha/\epsilon}, \quad (\text{B.19})$$

where $\epsilon \ll 1$. To leading order in ϵ we see that

$$\mathcal{P}_J^I(k_\alpha) u_0^J = \left(\delta_J^I k_t + [F_J^I]^i k_i \right) \tilde{u}^J = 0. \quad (\text{B.20})$$

Nontrivial solutions to this equation exist only if $\det \mathcal{P}_J^I(k_\alpha) = 0$, that is only if the wave vector k_α is a characteristic vector. The corresponding functional solutions \tilde{u}^I are the eigenvectors to $[F_J^I]^i \xi_i$, and are advected along the characteristics. Thus the wave fronts of high-frequency small amplitude solutions propagate on the characteristic surfaces. We also see that any low-amplitude, high frequency solution can be locally be written as a linear combination of the eigenvectors, provided the system is strongly hyperbolic.

Appendix C. Mixed-type partial differential equations

For completeness, here we review *mixed-type* PDE. Mixed-type PDE are PDE which have degrees of freedom which can change character from being hyperbolic to being elliptic in different solution regions; for general reviews see 132, 133, 136.

Appendix C.1. Two-dimensional PDE

Mixed-type PDE are differential equations that are neither hyperbolic nor elliptic over their entire solution domain.^{132, 133} The simplest examples of mixed-type PDE arise in two dimensions, and much that is formally known about these theories appear in this context. For these reasons we will focus mostly on two-dimensional mixed-type equations.

We first review some terminology.⁶¹ Consider PDE of the form

$$\begin{aligned} \mathcal{A}(x, y, u, \partial_x u, \partial_y u) \partial_x^2 u(x, y) + \mathcal{B}(x, y, u, \partial_x u, \partial_y u) \partial_x \partial_y u(x, y) \\ + \mathcal{C}(x, y, u, \partial_x u, \partial_y u) \partial_y^2 u(x, y) + \mathcal{F}(x, y, u, \partial_x u, \partial_y u) = 0. \end{aligned} \quad (\text{C.1})$$

The characteristic equation is

$$\mathcal{A}\xi_x^2 + \mathcal{B}\xi_x \xi_y + \mathcal{C}\xi_y^2 = 0. \quad (\text{C.2})$$

Following the discussion in Appendix B, we see that the theory is hyperbolic provided we can find two real solutions to this equation. This in turn is dictated by the *discriminant*, which is defined to be

$$\mathcal{D} \equiv \mathcal{B}^2 - 4\mathcal{A}\mathcal{C}. \quad (\text{C.3})$$

Consider a point (x, y) , and say we have specified $u, \partial_x u, \partial_y u$ at that point. We say that Eq. (C.1) is *hyperbolic* if $\mathcal{D} > 0$, *parabolic* if $\mathcal{D} = 0$, and *elliptic* if $\mathcal{D} < 0$. The classic examples of hyperbolic, parabolic, and elliptic PDEs in two dimensions are

$$\partial_x^2 u - \partial_y^2 u = 0, \quad (\text{C.4a})$$

$$\partial_x u - \partial_y^2 u = 0, \quad (\text{C.4b})$$

$$\partial_x^2 u + \partial_y^2 u = 0. \quad (\text{C.4c})$$

Locally we can transform any hyperbolic, parabolic, and elliptic equation to take the forms (C.4) through coordinate transformations.

The canonical examples of mixed-type PDE are the Tricomi and Keldysh equations,¹³¹ which respectively are

$$\partial_x^2 u(x, y) + x \partial_y^2 u(x, y) = 0, \quad (\text{C.5})$$

$$\partial_x^2 u(x, y) + \frac{1}{x} \partial_y^2 u(x, y) = 0. \quad (\text{C.6})$$

These equations are hyperbolic/parabolic/elliptic when $x < 0 / x = 0 / x > 0$. The hyperbolic and elliptic regions are separated by the parabolic *sonic line*^o. Locally we can transform mixed-type PDE near their sonic lines into either a Tricomi or Keldysh form.

The main qualitative differences between these two equations are how the characteristics in the hyperbolic region meet the parabolic sonic line, and how the characteristic speeds become imaginary. Treating x as the “time” variable, the characteristic velocities for the Tricomi and Keldysh equations respectively are

$$c_y^{Tri, \pm} = \pm (-x)^{1/2}, \quad c_y^{Kel, \pm} = \pm (-x)^{-1/2}. \quad (\text{C.7})$$

The integral curves of these then are

$$y^{Tri, \pm} = c \mp \frac{2}{3} (-x)^{3/2}, \quad y^{Kel, \pm} = c \mp 2 (-x)^{1/2}, \quad (\text{C.8})$$

which we plot in Fig. 2. For the Tricomi equation, the characteristics intersect the sonic line orthogonally, with the corresponding speeds going imaginary passing through zero there. For the Keldysh equation, the characteristics intersect the sonic line tangentially, with the characteristic speeds diverging there before becoming imaginary. These properties affect the degree of smoothness one can generally expect for solutions to these equations, with the Keldysh equation having weaker regularity of solutions on the sonic line.¹³³

^oThis terminology comes from hydrodynamics, which is the physical context in which mixed-type PDE were first studied.^{136,209} See also 210 for a discussion of numerical methods to solve mixed-type equations as they appear in hydrodynamics.

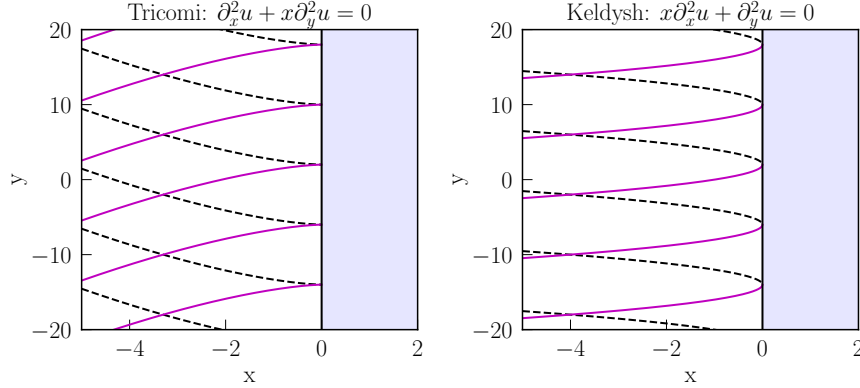


Fig. 2. The dash black and solid purple lines are the integral curves for the characteristics. The elliptic region $x > 0$ is shaded in light blue, and the sonic line $x = 0$ is the solid black vertical line. We see that the characteristic integral curves for the Tricomi equation intersect the sonic perpendicularly, while the characteristic integral curves for the Tricomi equation tangentially intersect the sonic line. Thus the characteristic speeds blow up before reaching the sonic line for the Keldysh equation. For more discussion see Morawetz¹³⁰ or Otway.¹³³

Appendix C.2. *Systems of PDE in higher dimensions*

We consider systems of first order PDE of the form Eq. (B.1). The characteristic equation is (see Appendix B)

$$\det(\mathcal{P}_J^I(\xi_\alpha)) = 0. \quad (\text{C.9})$$

We recall the characteristic equation is defined locally with respect to a location and solution: (x_0^α, u_0^I) . We say that the system (B.1) is

- (1) *hyperbolic* provided the characteristic equation has all real roots for all possible solutions over the entire domain
- (2) *elliptic* if the characteristic equation has all imaginary roots for all possible solutions over the entire domain.
- (3) *mixed-type* PDE if the roots can be real or imaginary depending on the solution/where in the domain you are

We define the sonic line to define the boundary between elliptic and hyperbolic domains. There are very few general results on systems of higher dimensional mixed-type PDE.

Appendix C.3. *Example of a mixed-type PDE from Horndeski gravity*

We conclude with an example of a mixed-type system of PDE in a higher-dimensional spacetime. We consider k-essence in fixed Minkowski spacetime,^{92, 93, 211} which is simply the \mathcal{G}_2 Horndeski term with no gravity. The mixed-type properties

of this theory were first thoroughly studied by Bernard et. al.²⁷ (see also Refs. 93, 128, 135). Focusing just on the scalar part of the action, we have

$$S_{(\phi)} = \int d^4 \sqrt{-\eta} K(X). \quad (\text{C.10})$$

The equations of motion are

$$(K' \eta^{\mu\nu} - K'' \partial^\mu \phi \partial^\nu \phi) \partial_\mu \partial_\nu \phi = 0. \quad (\text{C.11})$$

We define the variables

$$\Phi_\alpha \equiv \partial_\alpha \phi. \quad (\text{C.12})$$

We add to the equations of motion the integrability condition $\partial_0 \Phi_i = \partial_i \Phi_0$. From this it is straightforward to see that the constraint is propagated in time: if $C_i \equiv \partial_i \phi - \Phi_i = 0$ on a $t = 0$ initial data surface, then: $\partial_0 C_i = \partial_0 \partial_i \phi - \partial_0 \Phi_i = \partial_i \Phi_0 - \partial_0 \Phi_i = 0$. The equations of motion in these new variables are

$$\begin{bmatrix} (K' + K'' \Phi_0^2) & 0 \\ 0 & \delta_j^i \end{bmatrix} \partial_0 - \begin{pmatrix} 2K'' \Phi_0 \Phi^j & K' \eta^{ij} - K'' \Phi^i \Phi^j \\ 1 & 0 \end{pmatrix} \partial_j \begin{pmatrix} \Phi_0 \\ \Phi_i \end{pmatrix} = 0. \quad (\text{C.13})$$

The principal symbol is

$$\mathcal{P} = \begin{pmatrix} (K' + K'' \Phi_0^2) \xi_0 - 2K'' \Phi_0 \Phi^j \xi_j & -K' \xi^i + K'' \Phi^i \Phi^j \xi_j \\ -\xi_j & \delta_j^i \xi_0 \end{pmatrix}. \quad (\text{C.14})$$

The determinant is

$$\det \mathcal{P} = [(K' + K'' \Phi_0^2) \xi_0^2 - 2K'' \Phi_0 \Phi^j \xi_j \xi_0 - K' \xi^i \xi_i + K'' \Phi^i \Phi^j \xi_i \xi_j] \xi_0^2. \quad (\text{C.15})$$

This has solutions

$$\xi_0^{(\pm)} = \frac{1}{K' + K'' \Phi_0^2} \left(K'' \Phi_0 \Phi^i \xi_i \pm \sqrt{(K' + K'' \Phi_0^2) K' \xi^i \xi_i} \right), \quad (\text{C.16})$$

$$\xi_0 = 0. \quad (\text{C.17})$$

The condition $\xi_0 = 0$ comes from the integrability condition $\partial_0 \Phi_i = \partial_i \Phi_0$. We see that the sign of the discriminant to the first equation determines if the “physical” (non-constraint and non constraint-violating) degree of freedom is hyperbolic or elliptic (we assume ξ_i is real so $\xi^i \xi_i > 0$):

$$(K' + K'' \Phi_0^2) K' \begin{cases} \geq 0 & \text{hyperbolic} \\ < 0 & \text{elliptic} \end{cases}. \quad (\text{C.18})$$

If $K'' = 0$, then this is always positive semidefinite. For example when $K = X$, the theory is always hyperbolic. Note that the “constraint” degrees of freedom are always hyperbolic (they satisfy $\xi_0 = 0$). Studies in spherically symmetric spacetimes, show that the solutions to K -essence theories can take on Tricomi-like or Keldysh-like character near the formation of an elliptic region, depending on the specific form of $K(X)$.^{27, 113, 135} For example, at least in spherically symmetric spacetimes

for couplings $\mathcal{G}_2(\phi, X) \equiv K(X)$, the solutions have Keldysh-like behavior near sonic lines if¹³⁵

$$1 - 2 \frac{K''}{K'} X > 0. \quad (\text{C.19})$$

Recently work suggests that the Keldysh-like behavior may be removed through a suitable choice of gauge.⁹⁴ We believe that it is unlikely that elliptic regions could be removed for all solutions to all Horndeski theories, although there is no rigorous proof that is the case.

We end by noting that in general the ellipticity of the equations of motion are unrelated to the classical energy conditions. For example, in the case of K -essence, the stress-energy tensor is

$$T_{\mu\nu} = K' \partial_\mu \phi \partial_\nu \phi + g_{\mu\nu} K. \quad (\text{C.20})$$

We consider the Null Energy Condition (NEC), which states that the stress-energy tensor is positive semidefinite when contracted on all null vectors: $T_{\mu\nu} k^\mu k^\nu \geq 0$, $\forall k^\mu$ s.t. $k^\mu k_\mu = 0$; this condition is used in the proofs of the black hole area law and singularity theorems.¹¹⁶ Letting k^μ be an arbitrary null vector, we have

$$T_{\mu\nu} k^\mu k^\nu = K' (k^\mu \partial_\mu \phi)^2. \quad (\text{C.21})$$

Thus the stress-energy tensor obeys the NEC if $K' \geq 0$. We see that this is a distinct condition from the hyperbolicity of the equations of motion (C.18). For example, if $K = -X$ then the NEC is always violated ($K' = -1$) (except when $\partial_\alpha \phi = 0$), but the theory remains hyperbolic ($(K')^2 > 0$). While there is no direct relation between the energy conditions and the classical well-posedness of the Horndeski theories, it is less clear if the quantized version of a given NEC violating theory/solution has well-posed evolution. For a relatively recent review, see 212.

Appendix D. General properties of the principal symbol for Horndeski gravity

We review some useful properties of the principal symbol for the Horndeski theories (or more generally, theories that have second order equations of motion and that have a covariant action^{31,36,42}).

Appendix D.1. Definitions

The action for Horndeski gravity theories can be written schematically as

$$S = \int d^4x \sqrt{-g} L(g_{\mu\nu}, \phi). \quad (\text{D.1})$$

The equations of motion are

$$E_{(g)}^{\mu\nu} \equiv \frac{1}{\sqrt{-g}} \frac{\delta S}{\delta g_{\mu\nu}}, \quad E_{(\phi)} \equiv \frac{1}{\sqrt{-g}} \frac{\delta S}{\delta \phi}. \quad (\text{D.2})$$

The principal symbol of the system (D.2) is

$$\mathcal{P}(\xi) \begin{pmatrix} \delta g_{\rho\sigma} \\ \delta\phi \end{pmatrix} \equiv \begin{pmatrix} P_{(gg)}^{\mu\nu\rho\sigma\alpha\beta} & P_{(g\phi)}^{\mu\nu\alpha\beta} \\ P_{(\phi g)}^{\rho\sigma\alpha\beta} & P_{(\phi\phi)}^{\alpha\beta} \end{pmatrix} \xi_\alpha \xi_\beta \begin{pmatrix} \delta g_{\rho\sigma} \\ \delta\phi \end{pmatrix}, \quad (\text{D.3})$$

where

$$\begin{aligned} P_{(gg)}^{\mu\nu\rho\sigma\alpha\beta} &\equiv \frac{\delta E_{(g)}^{\mu\nu}}{\delta(\partial_\alpha\partial_\beta g_{\rho\sigma})}, & P_{(g\phi)}^{\mu\nu\alpha\beta} &\equiv \frac{\delta E_{(g)}^{\mu\nu}}{\delta(\partial_\alpha\partial_\beta\phi)}, \\ P_{(\phi g)}^{\rho\sigma\alpha\beta} &\equiv \frac{\delta E_{(\phi)}^{\rho\sigma}}{\delta(\partial_\alpha\partial_\beta g_{\rho\sigma})}, & P_{(\phi\phi)}^{\alpha\beta} &\equiv \frac{\delta E_{(\phi)}^{\alpha\beta}}{\delta(\partial_\alpha\partial_\beta\phi)}. \end{aligned}$$

Appendix D.2. General symmetries of the principal symbol

From the definitions in (D.3) we see that

$$P_{(gg)}^{\mu\nu\rho\sigma\alpha\beta} = P_{(gg)}^{(\mu\nu)\rho\sigma\alpha\beta} = P_{(gg)}^{\mu\nu(\rho\sigma)\alpha\beta} = P_{(gg)}^{\mu\nu\rho\sigma(\alpha\beta)}, \quad (\text{D.5a})$$

$$P_{(g\phi)}^{\mu\nu\alpha\beta} = P_{(g\phi)}^{(\mu\nu)\alpha\beta} = P_{(g\phi)}^{\mu\nu(\alpha\beta)}, \quad (\text{D.5b})$$

$$P_{(\phi g)}^{\rho\sigma\alpha\beta} = P_{(\phi g)}^{(\rho\sigma)\alpha\beta} = P_{(\phi g)}^{\rho\sigma(\alpha\beta)}, \quad (\text{D.5c})$$

$$P_{(\phi\phi)}^{\alpha\beta} = P_{(\phi\phi)}^{(\alpha\beta)}. \quad (\text{D.5d})$$

From the fact that the equations of motion are derived from an action, the principal symbol is a symmetric matrix⁴²

$$P_{(gg)}^{\mu\nu\rho\sigma\alpha\beta} = P_{(gg)}^{\rho\sigma\mu\nu\alpha\beta}, \quad (\text{D.6a})$$

$$P_{(g\phi)}^{\mu\nu\alpha\beta} = P_{(\phi g)}^{\mu\nu\alpha\beta}. \quad (\text{D.6b})$$

We next consider the additional symmetries that come from the action being covariant (diffeomorphism invariant). That is, the physical content of the equations of motion are left invariant by the transformations:

$$\delta g_{\mu\nu} \rightarrow \delta g_{\mu\nu} + 2\nabla_{(\mu} X_{\nu)}, \quad \delta\phi \rightarrow \delta\phi + X^\mu \nabla_\mu \phi, \quad (\text{D.7})$$

where X^μ is a real vector field. Diffeomorphism invariance implies the Bianchi identity

$$\nabla_\mu E_{(g)}^{\mu\nu} - E_{(\phi)} \nabla^\nu \phi = 0. \quad (\text{D.8})$$

To leading order in derivatives this is equal to

$$P_{(gg)}^{\mu\nu\rho\sigma\alpha\beta} \partial_\mu \partial_\alpha \partial_\beta g_{\rho\sigma} + P_{(g\phi)}^{\mu\nu\alpha\beta} \partial_\mu \partial_\alpha \partial_\beta \phi + l.o.t. = 0. \quad (\text{D.9})$$

Demanding that the highest derivative terms be zero, we have

$$P_{(gg)}^{(\mu|\nu\rho\sigma|\alpha\beta)} = 0, \quad (\text{D.10a})$$

$$P_{(g\phi)}^{(\mu|\nu|\alpha\beta)} = 0. \quad (\text{D.10b})$$

Appendix D.3. The main theorem about the principal symbol

Using these symmetries and much rearranging of indices, one can prove the following

Theorem (Reall³⁶) The principal symbol components can be written as

$$P_{(\phi g)}^{\mu\nu\alpha\beta}\xi_\alpha\xi_\beta = C^{\mu\alpha\nu\beta}\xi_\alpha\xi_\beta, \quad (\text{D.11})$$

$$P_{(gg)}^{\mu\nu\rho\sigma\alpha\beta}\xi_\alpha\xi_\beta = C^{\mu(\rho|\alpha\nu|\sigma)\beta}\xi_\alpha\xi_\beta, \quad (\text{D.12})$$

where $C^{\mu\nu\rho\sigma}$ has the same symmetries as the Riemann tensor

$$C^{\mu\nu\rho\sigma} = C^{[\mu\nu]\rho\sigma} = C^{\mu\nu[\rho\sigma]} = C^{\mu[\nu\rho\sigma]}, \quad (\text{D.13})$$

and $C^{\alpha_1\alpha_2\alpha_3\beta_1\beta_2\beta_3}$ has the symmetries

$$C^{\alpha_1\alpha_2\alpha_3\beta_1\beta_2\beta_3} = C^{[\alpha_1\alpha_2\alpha_3]\beta_1\beta_2\beta_3} = C^{\alpha_1\alpha_2\alpha_3[\beta_1\beta_2\beta_3]} = C^{\beta_1\beta_2\beta_3\alpha_1\alpha_2\alpha_3}, \quad (\text{D.14a})$$

$$C^{\alpha_1\alpha_2[\alpha_3\beta_1\beta_2\beta_3]} = C^{\alpha_1[\alpha_2\alpha_3\beta_1\beta_2\beta_3]} = 0. \quad (\text{D.14b})$$

These “C-tensors” are functions of $(g_{\mu\nu}, \phi)$ and their first and second derivatives.

From all the symmetries (D.13) (D.14), we see that we can write $C^{\alpha_1\alpha_2\alpha_3\beta_1\beta_2\beta_3}$ in terms of a symmetric two-tensor which we call $C_{\mu\nu}$ (this only holds in four spacetime dimensions):

$$C^{\alpha_1\alpha_2\alpha_3\beta_1\beta_2\beta_3} = -\frac{1}{2}\epsilon^{\alpha_1\alpha_2\alpha_3\mu}\epsilon^{\beta_1\beta_2\beta_3\nu}C_{\mu\nu}. \quad (\text{D.15})$$

Putting everything together then, the principal symbol for Horndeski can be written as

$$P(\xi) \begin{pmatrix} \delta g_{\rho\sigma} \\ \delta\phi \end{pmatrix} = \begin{pmatrix} -\frac{1}{2}\epsilon^{\mu\rho\alpha\kappa}\epsilon^{\nu\sigma\beta\lambda}C_{\kappa\lambda} & C^{\mu\nu\alpha\beta} \\ C^{\mu\nu\alpha\beta} & P_{(\phi\phi)}^{\alpha\beta} \end{pmatrix} \xi_\alpha\xi_\beta \begin{pmatrix} \delta g_{\rho\sigma} \\ \delta\phi \end{pmatrix}. \quad (\text{D.16})$$

For general relativity (with minimally coupled fields), $C^{\mu\nu\alpha\beta} = 0$ and $C^{\mu\nu} = g^{\mu\nu}$. This means for weakly-coupled solutions to the Horndeski theories, we expect $C^{\mu\nu\alpha\beta}$ to be “close” to zero and $C^{\mu\nu}$ to be “close” to $g^{\mu\nu}$.

Appendix D.4. Physical characteristics and the lack of second time derivatives in the constraint equations

A real covector ξ_μ is characteristic iff there exists a nonzero field configuration $\mathbf{z} \equiv (w_{\mu\nu}, v)$ such that $\mathcal{P}(\xi)\mathbf{z} = 0$. Due to the diffeomorphism invariance of the equations of motion, the following field configuration

$$w_{\mu\nu} = \xi_{(\mu}X_{\nu)}, \quad v = 0, \quad (\text{D.17})$$

solves $\mathcal{P}(\xi)\mathbf{z} = 0$ for all ξ_μ . We can “mod-out” these unphysical modes by considering equivalence classes of solutions. That is we only consider solutions that are the same up to the transformation⁶⁴

$$[w_{\mu\nu}] = \{t_{\mu\nu} : \exists \xi_\mu \text{ s.t. } t_{\mu\nu} = w_{\mu\nu} + \xi_{(\mu}X_{\nu)}\}. \quad (\text{D.18})$$

We can then think of the principal symbol as having the physical eigenvectors $[\mathbf{z}] = ([w_{\mu\nu}], v)$.

We next present a more general argument that shows the constraint equations have no second time derivatives acting on the fields in adapted ADM coordinates. As was shown by Reall³⁶ (see Appendix D.3), the principal part of the tensor equations of motion can be written as

$$\left(E^{(g)} \right)^{\mu\nu} = C^{\mu(\rho|\alpha\nu|\sigma)\beta} \partial_\alpha \partial_\beta g_{\rho\sigma} + C^{\mu\alpha\nu\beta} \partial_\alpha \partial_\beta \phi_I + l.o.t., \quad (\text{D.19})$$

where $C^{\mu\alpha\nu\beta}$ has the same symmetries as the Riemann tensor, and $C^{\mu(\rho|\alpha\nu|\sigma)\beta}$ has the following symmetries:

$$C^{\alpha_1\alpha_2\alpha_3\beta_1\beta_2\beta_3} = C^{[\alpha_1\alpha_2\alpha_3]\beta_1\beta_2\beta_3} = C^{\alpha_1\alpha_2\alpha_3[\beta_1\beta_2\beta_3]} = C^{\beta_1\beta_2\beta_3\alpha_1\alpha_2\alpha_3}, \quad (\text{D.20a})$$

$$C^{\alpha_1\alpha_2[\alpha_3\beta_1\beta_2\beta_3]} = C^{\alpha_1[\alpha_2\alpha_3\beta_1\beta_2\beta_3]} = 0. \quad (\text{D.20b})$$

In ADM coordinates we have $n_\mu = -N\delta_\mu^0$ (where N is the lapse; see Eq. (49)), so that

$$\begin{aligned} \mathcal{H} &= n_\mu n_\nu \left(C^{\mu(\rho|\alpha\nu|\sigma)\beta} \partial_\alpha \partial_\beta g_{\rho\sigma} + C^{\mu\alpha\nu\beta} \partial_\alpha \partial_\beta \phi \right) + l.o.t., \\ &= N^2 \left(C^{0(\rho|\alpha 0|\sigma)\beta} \partial_\alpha \partial_\beta g_{\rho\sigma} + C^{0\alpha 0\beta} \partial_\alpha \partial_\beta \phi \right) + l.o.t., \end{aligned} \quad (\text{D.21a})$$

$$\begin{aligned} \mathcal{M}_\mu &= n_\mu h_{\nu\gamma} \left(C^{\mu(\rho|\alpha\gamma|\sigma)\beta} \partial_\alpha \partial_\beta g_{\rho\sigma} + C^{\mu\alpha\nu\beta} \partial_\alpha \partial_\beta \phi \right) + l.o.t. \\ &= -N h_{\nu\gamma} \left(C^{0(\rho|\alpha\gamma|\sigma)\beta} \partial_\alpha \partial_\beta g_{\rho\sigma} + C^{0\alpha\nu\beta} \partial_\alpha \partial_\beta \phi \right) + l.o.t.. \end{aligned} \quad (\text{D.21b})$$

From the symmetries of the tensors $C^{\alpha_1\alpha_2\beta_1\beta_2}$ and $C^{\alpha_1\alpha_2\alpha_3\beta_1\beta_2\beta_3}$, we see that the terms with ∂_0^2 acting on the tensor or scalar field are zero.

Appendix E. Identities for the 3 + 1 decomposition of spacetime, and conformal transverse-traceless decomposition

Here we collect a few formulas that are useful for the 1 + 3 decomposition of the equations of motion, and the conformal transverse-traceless decomposition of the constraint equations. We refer to Sec. 8 for definitions.

The nonzero contractions of the Riemann tensor are^{2,158,213}

$$h_{\alpha_1}^{\mu_1} h_{\alpha_2}^{\mu_2} h_{\alpha_3}^{\mu_3} h_{\alpha_4}^{\mu_4} R_{\mu_1\mu_2\mu_3\mu_4} = {}^{(3)}R_{\alpha_1\alpha_2\alpha_3\alpha_4} + K_{\alpha_1\alpha_3} K_{\alpha_2\alpha_4} - K_{\alpha_1\alpha_4} K_{\alpha_2\alpha_3}, \quad (\text{E.1a})$$

$$h_{\alpha_1}^{\mu_1} h_{\alpha_2}^{\mu_2} h_{\alpha_3}^{\mu_3} n^{\mu_4} R_{\mu_1\mu_2\mu_3\mu_4} = D_{\alpha_2} K_{\alpha_1\alpha_3} - D_{\alpha_1} K_{\alpha_2\alpha_3}, \quad (\text{E.1b})$$

$$h_{\alpha_1}^{\mu_1} n^{\mu_2} h_{\alpha_3}^{\mu_3} n^{\mu_4} R_{\mu_1\mu_2\mu_3\mu_4} = \mathcal{L}_n K_{\alpha_1\alpha_3} + \frac{1}{N} D_{\alpha_1} D_{\alpha_3} N + K_{\alpha_1}^\gamma K_{\alpha_2\gamma}. \quad (\text{E.1c})$$

Similarly the nonzero contractions on the scalar field second derivatives are

$$h_\mu^\gamma h^\nu_\delta \nabla_\gamma \nabla^\delta \phi = D_\mu D^\nu \phi + n^\nu K_\mu^\delta D_\delta \phi + K_\mu^\nu \mathcal{L}_n \phi, \quad (\text{E.2})$$

$$h_\mu^\gamma n_\delta \nabla_\gamma \nabla^\delta \phi = D_\mu (\mathcal{L}_n \phi) + K_\mu^\delta D_\delta \phi, \quad (\text{E.3})$$

$$n^\gamma n_\delta \nabla_\gamma \nabla^\delta \phi = \mathcal{L}_n \mathcal{L}_n \phi - (n^\gamma \nabla_\gamma n^\delta) \nabla_\delta \phi, \quad (\text{E.4})$$

Where \mathcal{L}_n denotes the Lie derivative along n^μ .

We next list a few useful formulas for the CTT decomposition.^{34,213} The CTT decomposition rewrites the spatial metric as

$$h_{ij} = \psi^4 \tilde{h}_{ij}. \quad (\text{E.5})$$

We denote the metric compatible derivative with respect to h_{ij} as D_i , and the metric compatible derivative with respect to \tilde{h}_{ij} as \tilde{D}_i . We similarly denote the Christoffel symbols and Riemann tensor with respect to each metric. We have

$$\begin{aligned} {}^{(3)}\Gamma_{ij}^k &= {}^{(3)}\tilde{\Gamma}_{ij}^k + C_{ij}^k \\ &\equiv {}^{(3)}\tilde{\Gamma}_{ij}^k + 2 \left(\delta_i^k \tilde{D}_j \ln \psi + \delta_j^k \tilde{D}_i \ln \psi - \tilde{h}_{ij} \tilde{D}^k \ln \psi \right) \end{aligned} \quad (\text{E.6a})$$

$$\begin{aligned} {}^{(3)}R^{i_1 i_2}_{\quad j_1 j_2} &= \frac{1}{\psi^4} {}^{(3)}\tilde{R}^{i_1 i_2}_{\quad j_1 j_2} + 2 \frac{1}{\psi^4} \tilde{h}^{i_2 k} \tilde{D}_{[j_1} C_{j_2]k}^{i_1} + 2 \frac{1}{\psi^4} \tilde{h}^{i_2 k} C_{l[j_1}^{i_2} C_{j_2]k}^l \\ &= \frac{1}{\psi^4} {}^{(3)}\tilde{R}^{i_1 i_2}_{\quad j_1 j_2} - 8 \frac{1}{\psi^5} \delta_{[j_1}^{[i_1} \tilde{D}_{j_2]} \tilde{D}^{i_2]} \psi \\ &\quad + 24 \frac{1}{\psi^6} \delta_{[j_1}^{[i_1} \tilde{D}_{i_2]} \psi \tilde{D}^{i_2]} \psi - 4 \delta_{j_1 j_2}^{i_1 i_2} \tilde{D}_k \psi \tilde{D}^k \psi. \end{aligned} \quad (\text{E.6b})$$

Appendix F. $4\partial ST$ gravity as a gradient expansion about General Relativity with a scalar field

Here we review an effective field theory/gradient expansion-styled argument to motivate $4\partial ST$ gravity.^{30,31,214} We assume a zeroeth order action

$$S_0 = \int d^4x \sqrt{-g} \left(\frac{1}{2} R + X - V(\phi) \right). \quad (\text{F.1})$$

Assuming a gradient expansion about this action, the leading order corrections to (F.1) will contain all of the covariant terms with four spacetime derivatives and order-unity coefficients (there can be no third covariant terms with only three derivatives in a $4D$ spacetime). Up to total derivatives and integration by parts, these are

$$\begin{aligned} S_{\partial^4} = \int d^4x \sqrt{-g} &\left(f_1(\phi) X^2 + f_2(\phi) X \square \phi + f_3(\phi) (\square \phi)^2 \right. \\ &\quad + f_4(\phi) R^{\mu\nu} \nabla_\mu \phi \nabla_\nu \phi + f_5(\phi) R X + f_6(\phi) R \square \phi \\ &\quad + f_7(\phi) R^2 + f_8(\phi) R^{\mu\nu} R_{\mu\nu} \\ &\quad \left. + f_9(\phi) \mathcal{R}_{GB} + f_{10}(\phi) \mathcal{R}_P \right). \end{aligned} \quad (\text{F.2})$$

The four dimensional Gauss-Bonnet scalar \mathcal{R}_{GB} and the Pontryagin density \mathcal{R}_P are

$$\mathcal{R}_{GB} \equiv \frac{1}{4} \delta_{\alpha\beta\gamma\delta}^{\mu\nu\rho\sigma} R^{\alpha\beta}_{\mu\nu} R^{\gamma\delta}_{\rho\sigma}, \quad (\text{F.3})$$

$$\mathcal{R}_P \equiv \frac{1}{2} \epsilon^{\gamma\delta\mu\nu} R^{\alpha\beta}_{\mu\nu} R_{\beta\alpha\gamma\delta}, \quad (\text{F.4})$$

where $\delta^{\alpha\beta\gamma\delta}$ is the generalized Kronecker delta tensor and $\epsilon^{\mu\nu\gamma\delta}$ is the Levi-Cevita tensor. Besides using X instead of $(\nabla\phi)^2$, the action (F.2) differs from Weinberg's²¹⁴ Eq. (3) in that we use the Gauss-Bonnet scalar \mathcal{R}_{GB} instead of the contraction of the Weyl tensor: $C_{\mu\nu\alpha\beta}C^{\mu\nu\alpha\beta}$ (the Pontryagin density can be written equivalently in terms of contractions of the Weyl tensor²¹⁵). Up to field redefinitions and total derivatives, these two terms can be interchanged with one another.^{30,31}

If we were to consider the equations of motion in Eq. (F.2), the equations of motion would be fourth order in time for both the tensor and scalar field, which would imply there are two new degrees of freedom. We must remove these two “spurious” degrees of freedom in order for the solution to be consistent with the gradient expansion. This is accomplished by using the lower order equations of motion to remove higher derivative terms. This can be done several ways:

- (1) By removing higher derivative terms directly in the action by using the lower-order equations of motion.
- (2) By removing the higher derivative terms in the equations of motion by making use of the lower-order equations of motion.
- (3) By solving the full system of equations of motion order-by-order in a small expansion parameter (order-reduction methods).

Following Weinberg, we focus on the first approach. The lower-order equations of motion are found by varying Eq. (F.1) to obtain:

$$R_{\mu\nu} - \nabla_\mu\phi\nabla_\nu\phi - g_{\mu\nu}V = 0, \quad (\text{F.5})$$

$$\square\phi - V' = 0. \quad (\text{F.6})$$

With these equations we can remove all higher derivative terms that have powers of $R_{\mu\nu}$, R and $\square\phi$. Relabeling things, we see that the final action can be written as

$$S = \int d^4x \sqrt{-g} \left(\frac{1}{2}R + X - V(\phi) + \alpha(\phi)X^2 + \beta(\phi)\mathcal{R}_{GB} + \gamma(\phi)\mathcal{R}_P \right). \quad (\text{F.7})$$

The Pontryagin density is not invariant under parity $\mathbf{x} \rightarrow -\mathbf{x}$; if $\gamma \neq 0$ then we would need ϕ to be a pseudoscalar and the couplings to take a particular form if we wanted the action to be invariant under parity.⁸⁴ If we assume ϕ is a scalar, and that the action is invariant under parity transforms, we are left with $4\partial ST$ gravity:

$$S_{4\partial ST} = \int d^4x \sqrt{-g} \left(\frac{1}{2}R + X - V(\phi) + \alpha(\phi)X^2 + \beta(\phi)\mathcal{R}_{GB} \right). \quad (\text{F.8})$$

This action has second order equations of motion, so the higher derivative terms do not induce new degrees of freedom. Thus in $4\partial ST$ gravity we can solve the full equations of motion and obtain a solution consistent with the gradient expansion, provided the higher derivative terms make a suitable “small” contribution to the solution.^{30,31} If we had kept the Pontryagin term, the equations of motion would not be second order.⁸⁵ Order-reductions methods are currently being developed for application in numerical relativity to solve for the dynamics of theories that have the scalar field-Pontryagin coupling.^{86–88,155}

References

1. M. Alcubierre. *Introduction to 3+1 Numerical Relativity*. International Series of Monographs on Physics. OUP Oxford, 2008.
2. T.W. Baumgarte and S.L. Shapiro. *Numerical Relativity: Solving Einstein's Equations on the Computer*. Cambridge University Press, 2010.
3. Frans Pretorius. Evolution of binary black hole spacetimes. *Phys. Rev. Lett.*, 95:121101, 2005, gr-qc/0507014.
4. Manuela Campanelli, C. O. Lousto, P. Marronetti, and Y. Zlochower. Accurate evolutions of orbiting black-hole binaries without excision. *Phys. Rev. Lett.*, 96:111101, 2006, gr-qc/0511048.
5. John G. Baker, Joan Centrella, Dae-Il Choi, Michael Koppitz, and James van Meter. Gravitational wave extraction from an inspiraling configuration of merging black holes. *Phys. Rev. Lett.*, 96:111102, 2006, gr-qc/0511103.
6. Frans Pretorius. Binary Black Hole Coalescence. 8 2007, 0710.1338.
7. B. P. Abbott et al. Observation of Gravitational Waves from a Binary Black Hole Merger. *Phys. Rev. Lett.*, 116(6):061102, 2016, 1602.03837.
8. B. P. Abbott et al. GW151226: Observation of Gravitational Waves from a 22-Solar-Mass Binary Black Hole Coalescence. *Phys. Rev. Lett.*, 116(24):241103, 2016, 1606.04855.
9. B. P. Abbott et al. GW170817: Observation of Gravitational Waves from a Binary Neutron Star Inspiral. *Phys. Rev. Lett.*, 119(16):161101, 2017, 1710.05832.
10. Nicolás Yunes and Xavier Siemens. Gravitational-Wave Tests of General Relativity with Ground-Based Detectors and Pulsar Timing-Arrays. *Living Rev. Rel.*, 16:9, 2013, 1304.3473.
11. Emanuele Berti et al. Testing General Relativity with Present and Future Astrophysical Observations. *Class. Quant. Grav.*, 32:243001, 2015, 1501.07274.
12. Francois Foucart, Pablo Laguna, Geoffrey Lovelace, David Radice, and Helvi Witek. Snowmass2021 Cosmic Frontier White Paper: Numerical relativity for next-generation gravitational-wave probes of fundamental physics. 3 2022, 2203.08139.
13. B. P. Abbott et al. Tests of general relativity with GW150914. *Phys. Rev. Lett.*, 116(22):221101, 2016, 1602.03841. [Erratum: Phys.Rev.Lett. 121, 129902 (2018)].
14. B. P. Abbott et al. Tests of General Relativity with the Binary Black Hole Signals from the LIGO-Virgo Catalog GWTC-1. *Phys. Rev. D*, 100(10):104036, 2019, 1903.04467.
15. R. Abbott et al. Tests of general relativity with binary black holes from the second LIGO-Virgo gravitational-wave transient catalog. *Phys. Rev. D*, 103(12):122002, 2021, 2010.14529.
16. N. V. Krishnendu and Frank Ohme. Testing General Relativity with Gravitational Waves: An Overview. *Universe*, 7(12):497, 2021, 2201.05418.
17. Gregory Walter Horndeski. Second-Order Scalar-Tensor Field Equations in a Four-Dimensional Space. *International Journal of Theoretical Physics*, 10(6):363–384, September 1974.
18. C. Deffayet, Gilles Esposito-Farese, and A. Vikman. Covariant Galileon. *Phys. Rev. D*, 79:084003, 2009, 0901.1314.
19. C. Deffayet, Xian Gao, D. A. Steer, and G. Zahariade. From k-essence to generalised Galileons. *Phys. Rev. D*, 84:064039, 2011, 1103.3260.
20. Thibault Damour and Gilles Esposito-Farese. Nonperturbative strong field effects in tensor - scalar theories of gravitation. *Phys. Rev. Lett.*, 70:2220–2223, 1993.
21. P. Kanti, N. E. Mavromatos, J. Rizos, K. Tamvakis, and E. Winstanley. Dilatonic black holes in higher curvature string gravity. *Phys. Rev. D*, 54:5049–5058, 1996,

hep-th/9511071.

22. Thomas P. Sotiriou and Shuang-Yong Zhou. Black hole hair in generalized scalar-tensor gravity. *Phys. Rev. Lett.*, 112:251102, 2014, 1312.3622.
23. Edmund J. Copeland, M. Sami, and Shinji Tsujikawa. Dynamics of dark energy. *Int. J. Mod. Phys. D*, 15:1753–1936, 2006, hep-th/0603057.
24. T. Baker, E. Bellini, P. G. Ferreira, M. Lagos, J. Noller, and I. Sawicki. Strong constraints on cosmological gravity from GW170817 and GRB 170817A. *Phys. Rev. Lett.*, 119(25):251301, 2017, 1710.06394.
25. Juan Cayuso, Néstor Ortiz, and Luis Lehner. Fixing extensions to general relativity in the nonlinear regime. *Phys. Rev. D*, 96(8):084043, 2017, 1706.07421.
26. Gwyneth Allwright and Luis Lehner. Towards the nonlinear regime in extensions to GR: assessing possible options. *Class. Quant. Grav.*, 36(8):084001, 2019, 1808.07897.
27. Laura Bernard, Luis Lehner, and Raimon Luna. Challenges to global solutions in Horndeski’s theory. *Phys. Rev. D*, 100(2):024011, 2019, 1904.12866.
28. Áron D. Kovács. Well-posedness of cubic Horndeski theories. *Phys. Rev. D*, 100(2):024005, 2019, 1904.00963.
29. Helvi Witek, Leonardo Gualtieri, and Paolo Pani. Towards numerical relativity in scalar Gauss-Bonnet gravity: 3 + 1 decomposition beyond the small-coupling limit. *Phys. Rev. D*, 101(12):124055, 2020, 2004.00009.
30. Áron D. Kovács and Harvey S. Reall. Well-Posed Formulation of Scalar-Tensor Effective Field Theory. *Phys. Rev. Lett.*, 124(22):221101, 2020, 2003.04327.
31. Áron D. Kovács and Harvey S. Reall. Well-posed formulation of Lovelock and Horndeski theories. *Phys. Rev. D*, 101(12):124003, 2020, 2003.08398.
32. Richard P. Woodard. Ostrogradsky’s theorem on Hamiltonian instability. *Scholarpedia*, 10(8):32243, 2015, 1506.02210.
33. Tsutomu Kobayashi. Horndeski theory and beyond: a review. *Rept. Prog. Phys.*, 82(8):086901, 2019, 1901.07183.
34. Aron D. Kovacs. On the construction of asymptotically flat initial data in scalar-tensor effective field theory. 3 2021, 2103.06895.
35. Aron Kovacs. *The Cauchy problem and the initial data problem in effective theories of gravity*. PhD thesis, University of Cambridge, 2021.
36. Harvey S. Reall. Causality in gravitational theories with second order equations of motion. *Phys. Rev. D*, 103(8):084027, 2021, 2101.11623.
37. L. Rezzolla and O. Zanotti. *Relativistic Hydrodynamics*. EBSCO ebook academic collection. OUP Oxford, 2013.
38. Justin L. Ripley and Frans Pretorius. Hyperbolicity in Spherical Gravitational Collapse in a Horndeski Theory. *Phys. Rev. D*, 99(8):084014, 2019, 1902.01468.
39. Justin L. Ripley and Frans Pretorius. Gravitational collapse in Einstein dilaton-Gauss-Bonnet gravity. *Class. Quant. Grav.*, 36(13):134001, 2019, 1903.07543.
40. Pau Figueras and Tiago França. Gravitational Collapse in Cubic Horndeski Theories. *Class. Quant. Grav.*, 37(22):225009, 2020, 2006.09414.
41. William E. East and Justin L. Ripley. Dynamics of Spontaneous Black Hole Scalarization and Mergers in Einstein-Scalar-Gauss-Bonnet Gravity. *Phys. Rev. Lett.*, 127(10):101102, 2021, 2105.08571.
42. Giuseppe Papallo and Harvey S. Reall. On the local well-posedness of Lovelock and Horndeski theories. *Phys. Rev. D*, 96(4):044019, 2017, 1705.04370.
43. Barton Zwiebach. Curvature Squared Terms and String Theories. *Phys. Lett. B*, 156:315–317, 1985.
44. David J. Gross and John H. Sloan. The Quartic Effective Action for the Heterotic String. *Nucl. Phys. B*, 291:41–89, 1987.

45. Tsutomu Kobayashi, Masahide Yamaguchi, and Jun'ichi Yokoyama. Generalized G-inflation: Inflation with the most general second-order field equations. *Prog. Theor. Phys.*, 126:511–529, 2011, 1105.5723.
46. Thomas P. Sotiriou and Shuang-Yong Zhou. Black hole hair in generalized scalar-tensor gravity: An explicit example. *Phys. Rev. D*, 90:124063, 2014, 1408.1698.
47. Thomas P. Sotiriou. Black Holes and Scalar Fields. *Class. Quant. Grav.*, 32(21):214002, 2015, 1505.00248.
48. Hector O. Silva, Jeremy Sakstein, Leonardo Gualtieri, Thomas P. Sotiriou, and Emanuele Berti. Spontaneous scalarization of black holes and compact stars from a Gauss-Bonnet coupling. *Phys. Rev. Lett.*, 120(13):131104, 2018, 1711.02080.
49. Daniela D. Doneva and Stoytcho S. Yazadjiev. New Gauss-Bonnet Black Holes with Curvature-Induced Scalarization in Extended Scalar-Tensor Theories. *Phys. Rev. Lett.*, 120(13):131103, 2018, 1711.01187.
50. Masato Minamitsuji and Taishi Ikeda. Scalarized black holes in the presence of the coupling to Gauss-Bonnet gravity. *Phys. Rev. D*, 99(4):044017, 2019, 1812.03551.
51. Yasunori Fujii and Kei-ichi Maeda. *The Scalar-Tensor Theory of Gravitation*. Cambridge Monographs on Mathematical Physics. Cambridge University Press, 2003.
52. Clifford M. Will. *Theory and Experiment in Gravitational Physics*. Cambridge University Press, 2 edition, 2018.
53. Kei-ichi Maeda, Nobuyoshi Ohta, and Yukinori Sasagawa. Black Hole Solutions in String Theory with Gauss-Bonnet Curvature Correction. *Phys. Rev. D*, 80:104032, 2009, 0908.4151.
54. S. W. Hawking. Black holes in the Brans-Dicke theory of gravitation. *Commun. Math. Phys.*, 25:167–171, 1972.
55. Eanna E. Flanagan. The Conformal frame freedom in theories of gravitation. *Class. Quant. Grav.*, 21:3817, 2004, gr-qc/0403063.
56. Thibault Damour and Gilles Esposito-Farese. Tensor - scalar gravity and binary pulsar experiments. *Phys. Rev. D*, 54:1474–1491, 1996, gr-qc/9602056.
57. Clifford M. Will. The Confrontation between General Relativity and Experiment. *Living Rev. Rel.*, 17:4, 2014, 1403.7377.
58. Jacob D. Bekenstein. The Relation between physical and gravitational geometry. *Phys. Rev. D*, 48:3641–3647, 1993, gr-qc/9211017.
59. Miguel Zumalacárregui and Juan García-Bellido. Transforming gravity: from derivative couplings to matter to second-order scalar-tensor theories beyond the Horndeski Lagrangian. *Phys. Rev. D*, 89:064046, 2014, 1308.4685.
60. Dario Bettoni and Stefano Liberati. Disformal invariance of second order scalar-tensor theories: Framing the Horndeski action. *Phys. Rev. D*, 88:084020, 2013, 1306.6724.
61. L.C. Evans. *Partial Differential Equations*. Graduate studies in mathematics. American Mathematical Society, Providence, R.I., 2010.
62. Olivier Sarbach and Manuel Tiglio. Continuum and Discrete Initial-Boundary-Value Problems and Einstein's Field Equations. *Living Rev. Rel.*, 15:9, 2012, 1203.6443.
63. David Hilditch. An Introduction to Well-posedness and Free-evolution. *Int. J. Mod. Phys. A*, 28:1340015, 2013, 1309.2012.
64. D. Christodoulou. *Mathematical Problems of General Relativity I*. Mathematical Problems of General Relativity. European Mathematical Society, Zurich, 2008.
65. Oscar A. Reula. Hyperbolic Methods of Einstein's Equations. *Living Rev. Rel.*, 1:1433–8351, 1998.
66. Masaru Shibata and Takashi Nakamura. Evolution of three-dimensional gravitational waves: Harmonic slicing case. *Phys. Rev. D*, 52:5428–5444, 1995.

67. Thomas W. Baumgarte and Stuart L. Shapiro. On the numerical integration of Einstein's field equations. *Phys. Rev. D*, 59:024007, 1998, gr-qc/9810065.
68. H. Friedrich. Hyperbolic reductions for Einstein's equations. *Class. Quant. Grav.*, 13:1451–1469, 1996.
69. David Garfinkle. Harmonic coordinate method for simulating generic singularities. *Phys. Rev. D*, 65:044029, 2002, gr-qc/0110013.
70. Frans Pretorius. Simulation of binary black hole spacetimes with a harmonic evolution scheme. *Class. Quant. Grav.*, 23:S529–S552, 2006, gr-qc/0602115.
71. Y. Fourès-Bruhat. Théorème d'existence pour certains systèmes d'équations aux dérivées partielles non linéaires. *Acta Mathematica*, 88(1):141–225, January 1952.
72. Frans Pretorius. Numerical relativity using a generalized harmonic decomposition. *Class. Quant. Grav.*, 22:425–452, 2005, gr-qc/0407110.
73. Giuseppe Papallo. On the hyperbolicity of the most general Horndeski theory. *Phys. Rev. D*, 96(12):124036, 2017, 1710.10155.
74. Matthew W. Choptuik. Universality and scaling in gravitational collapse of a massless scalar field. *Phys. Rev. Lett.*, 70:9–12, 1993.
75. Justin L. Ripley and Frans Pretorius. Scalarized Black Hole dynamics in Einstein dilaton Gauss-Bonnet Gravity. *Phys. Rev. D*, 101(4):044015, 2020, 1911.11027.
76. Justin L. Ripley and Frans Pretorius. Dynamics of a \mathbb{Z}_2 symmetric EdGB gravity in spherical symmetry. *Class. Quant. Grav.*, 37(15):155003, 2020, 2005.05417.
77. Fabrizio Corelli, Marina De Amicis, Taishi Ikeda, and Paolo Pani. What is the fate of Hawking evaporation in gravity theories with higher curvature terms? 5 2022, 2205.13006.
78. Fabrizio Corelli, Marina De Amicis, Taishi Ikeda, and Paolo Pani. Nonperturbative gedanken experiments in Einstein-dilaton-Gauss-Bonnet gravity: nonlinear transitions and tests of the cosmic censorship beyond General Relativity. 5 2022, 2205.13007.
79. A.I. Vainshtein. To the problem of nonvanishing gravitation mass. *Physics Letters B*, 39(3):393–394, 1972.
80. Austin Joyce, Bhuvnesh Jain, Justin Khoury, and Mark Trodden. Beyond the Cosmological Standard Model. *Phys. Rept.*, 568:1–98, 2015, 1407.0059.
81. Helvi Witek, Leonardo Gualtieri, Paolo Pani, and Thomas P. Sotiriou. Black holes and binary mergers in scalar Gauss-Bonnet gravity: scalar field dynamics. *Phys. Rev. D*, 99(6):064035, 2019, 1810.05177.
82. Maria Okounkova. Stability of Rotating Black Holes in Einstein Dilaton Gauss-Bonnet Gravity. *Phys. Rev. D*, 100(12):124054, 2019, 1909.12251.
83. Maria Okounkova. Numerical relativity simulation of GW150914 in Einstein dilaton Gauss-Bonnet gravity. *Phys. Rev. D*, 102(8):084046, 2020, 2001.03571.
84. Stephon Alexander and Nicolas Yunes. Chern-Simons Modified General Relativity. *Phys. Rept.*, 480:1–55, 2009, 0907.2562.
85. Térence Delsate, David Hilditch, and Helvi Witek. Initial value formulation of dynamical Chern-Simons gravity. *Phys. Rev. D*, 91(2):024027, 2015, 1407.6727.
86. Maria Okounkova, Leo C. Stein, Mark A. Scheel, and Daniel A. Hemberger. Numerical binary black hole mergers in dynamical Chern-Simons gravity: Scalar field. *Phys. Rev. D*, 96(4):044020, 2017, 1705.07924.
87. Maria Okounkova, Mark A. Scheel, and Saul A. Teukolsky. Numerical black hole initial data and shadows in dynamical Chern-Simons gravity. *Class. Quant. Grav.*, 36(5):054001, 2019, 1810.05306.
88. Maria Okounkova, Mark A. Scheel, and Saul A. Teukolsky. Evolving Metric Perturbations in dynamical Chern-Simons Gravity. *Phys. Rev. D*, 99(4):044019, 2019,

1811.10713.

89. Solomon Endlich, Victor Gorbenko, Junwu Huang, and Leonardo Senatore. An effective formalism for testing extensions to General Relativity with gravitational waves. *JHEP*, 09:122, 2017, 1704.01590.
90. Ramiro Cayuso and Luis Lehner. Nonlinear, noniterative treatment of EFT-motivated gravity. *Phys. Rev. D*, 102(8):084008, 2020, 2005.13720.
91. C. Armendariz-Picon, Viatcheslav F. Mukhanov, and Paul J. Steinhardt. A Dynamical solution to the problem of a small cosmological constant and late time cosmic acceleration. *Phys. Rev. Lett.*, 85:4438–4441, 2000, astro-ph/0004134.
92. C. Armendariz-Picon, Viatcheslav F. Mukhanov, and Paul J. Steinhardt. Essentials of k essence. *Phys. Rev. D*, 63:103510, 2001, astro-ph/0006373.
93. Alan D. Rendall. Dynamics of k -essence. *Class. Quant. Grav.*, 23:1557–1570, 2006, gr-qc/0511158.
94. Miguel Bezares, Ricard Aguilera-Miret, Lotte ter Haar, Marco Crisostomi, Carlos Palenzuela, and Enrico Barausse. No Evidence of Kinetic Screening in Simulations of Merging Binary Neutron Stars beyond General Relativity. *Phys. Rev. Lett.*, 128(9):091103, 2022, 2107.05648.
95. C. Bona, T. Ledvinka, C. Palenzuela, and M. Zacek. General covariant evolution formalism for numerical relativity. *Phys. Rev. D*, 67:104005, 2003, gr-qc/0302083.
96. Daniela Alic, Carles Bona-Casas, Carles Bona, Luciano Rezzolla, and Carlos Palenzuela. Conformal and covariant formulation of the Z4 system with constraint-violation damping. *Phys. Rev. D*, 85:064040, 2012, 1106.2254.
97. Pau Figueras and Tiago França. Black Hole Binaries in Cubic Horndeski Theories. 12 2021, 2112.15529.
98. Robert V. Wagoner. Scalar tensor theory and gravitational waves. *Phys. Rev. D*, 1:3209–3216, 1970.
99. Kenneth Nordtvedt Jr. Post-newtonian metric for a general class of scalar-tensor gravitational theories and observational consequences. *The Astrophysical Journal*, 161:1059, 1970.
100. Israel Quiros. Selected topics in scalar–tensor theories and beyond. *Int. J. Mod. Phys. D*, 28(07):1930012, 2019, 1901.08690.
101. C. Brans and R. H. Dicke. Mach’s principle and a relativistic theory of gravitation. *Phys. Rev.*, 124:925–935, 1961.
102. Marcelo Salgado, David Martinez-del Rio, Miguel Alcubierre, and Dario Nunez. Hyperbolicity of scalar-tensor theories of gravity. *Phys. Rev. D*, 77:104010, 2008, 0801.2372.
103. Lotte ter Haar, Miguel Bezares, Marco Crisostomi, Enrico Barausse, and Carlos Palenzuela. Dynamics of Screening in Modified Gravity. *Phys. Rev. Lett.*, 126:091102, 2021, 2009.03354.
104. Miguel Bezares, Lotte ter Haar, Marco Crisostomi, Enrico Barausse, and Carlos Palenzuela. Kinetic screening in nonlinear stellar oscillations and gravitational collapse. *Phys. Rev. D*, 104(4):044022, 2021, 2105.13992.
105. Llibert Aresté Saló, Katy Clough, and Pau Figueras. Well-posedness of the four-derivative scalar-tensor theory of gravity in singularity avoiding coordinates. 8 2022, 2208.14470.
106. Carsten Gundlach, Jose M. Martin-Garcia, Gioel Calabrese, and Ian Hinder. Constraint damping in the Z4 formulation and harmonic gauge. *Class. Quant. Grav.*, 22:3767–3774, 2005, gr-qc/0504114.
107. William E. East and Justin L. Ripley. Evolution of Einstein-scalar-Gauss-Bonnet gravity using a modified harmonic formulation. *Phys. Rev. D*, 103(4):044040, 2021,

2011.03547.

108. W. Israel. Nonstationary irreversible thermodynamics: A Causal relativistic theory. *Annals Phys.*, 100:310–331, 1976.
109. W. Israel and J. M. Stewart. Thermodynamics of nonstationary and transient effects in a relativistic gas. *Physics Letters A*, 58(4):213–215, September 1976.
110. W. Israel and J. M. Stewart. Transient relativistic thermodynamics and kinetic theory. *Annals Phys.*, 118:341–372, 1979.
111. Eugeny Babichev. Formation of caustics in k-essence and Horndeski theory. *JHEP*, 04:129, 2016, 1602.00735.
112. Eugeny Babichev and Sabir Ramazanov. Caustic free completion of pressureless perfect fluid and k-essence. *JHEP*, 08:040, 2017, 1704.03367.
113. Guillermo Lara, Miguel Bezares, and Enrico Barausse. UV completions, fixing the equations, and nonlinearities in k-essence. *Phys. Rev. D*, 105(6):064058, 2022, 2112.09186.
114. Mary Gerhardinger, John T. Giblin, Andrew J. Tolley, and Mark Trodden. A Well-Posed UV Completion for Simulating Scalar Galileons. 5 2022, 2205.05697.
115. Nicola Franchini, Miguel Bezares, Enrico Barausse, and Luis Lehner. Fixing the dynamical evolution in scalar-Gauss-Bonnet gravity. 5 2022, 2206.00014.
116. S. W. Hawking and G. F. R. Ellis. *The Large Scale Structure of Space-Time*. Cambridge Monographs on Mathematical Physics. Cambridge University Press, 1973.
117. Demetrios Christodoulou. Examples of naked singularity formation in the gravitational collapse of a scalar field. *Annals of Mathematics*, 140(3):607–653, 1994.
118. Xuefeng Zhang and Xinliang An. Examples of naked singularity formation in higher-dimensional Einstein-vacuum spacetimes. *Annales Henri Poincaré*, 19(2):619–651, 2018, 1509.07956.
119. Demetrios Christodoulou. The instability of naked singularities in the gravitational collapse of a scalar field. *Annals of Mathematics*, 149(1):183–217, 1999.
120. Roger Penrose. Gravitational Collapse: the Role of General Relativity. *Nuovo Cimento Rivista Serie*, 1:252, January 1969.
121. Robert M. Wald. Gravitational collapse and cosmic censorship. pages 69–85, 10 1997, gr-qc/9710068.
122. G. Antoniou, A. Bakopoulos, and P. Kanti. Black-Hole Solutions with Scalar Hair in Einstein-Scalar-Gauss-Bonnet Theories. *Phys. Rev. D*, 97(8):084037, 2018, 1711.07431.
123. Burkhard Kleihaus, Jutta Kunz, Sindy Mojica, and Eugen Radu. Spinning black holes in Einstein–Gauss–Bonnet–dilaton theory: Nonperturbative solutions. *Phys. Rev. D*, 93(4):044047, 2016, 1511.05513.
124. Claudia de Rham and Hayato Motohashi. Caustics for Spherical Waves. *Phys. Rev. D*, 95(6):064008, 2017, 1611.05038.
125. Norihiro Tanahashi and Seiju Ohashi. Wave propagation and shock formation in the most general scalar–tensor theories. *Class. Quant. Grav.*, 34(21):215003, 2017, 1704.02757.
126. Klaountia Pasmatsiou. Caustic Formation upon Shift Symmetry Breaking. *Phys. Rev. D*, 97(3):036008, 2018, 1712.02888.
127. Jonathan Thornburg. Event and apparent horizon finders for 3+1 numerical relativity. *Living Rev. Rel.*, 10:3, 2007, gr-qc/0512169.
128. Ratindranath Akhoury, David Garfinkle, and Ryo Saotome. Gravitational collapse of k-essence. *JHEP*, 04:096, 2011, 1103.0290.
129. J M Stewart. Signature change, mixed problems and numerical relativity. *Classical and Quantum Gravity*, 18(23):4983–4995, nov 2001.

130. Cathleen S. Morawetz. The dirichlet problem for the tricomi equation. *Communications on Pure and Applied Mathematics*, 23(4):587–601, 1970, <https://onlinelibrary.wiley.com/doi/pdf/10.1002/cpa.3160230404>.
131. Gui-Qiang G. Chen. *Princeton Companion to Applied Mathematics*, chapter The Tricomi Equation. Princeton University Press, 2015, 1311.3338.
132. J.M. Rassias. *Lecture Notes on Mixed Type Partial Differential Equations*. Notas didáticas do ICMSC-USP. World Scientific, 1990.
133. T.H. Otway. *Elliptic–Hyperbolic Partial Differential Equations: A Mini-Course in Geometric and Quasilinear Methods*. SpringerBriefs in Mathematics. Springer International Publishing, 2015.
134. R.M. Wald. *General Relativity*. University of Chicago Press, 2010.
135. Miguel Bezares, Marco Crisostomi, Carlos Palenzuela, and Enrico Barausse. K-dynamics: well-posed 1+1 evolutions in K-essence. *JCAP*, 03:072, 2021, 2008.07546.
136. Cathleen Synge Morawetz. Mixed equations and transonic flow. *Journal of Hyperbolic Differential Equations*, 01(01):1–26, 2004, <https://doi.org/10.1142/S0219891604000081>.
137. C. Ferrari, F.G. Tricomi, and R.H. Cramer. *Transonic Aerodynamics*. Academic Press, 1968.
138. A.K. Aziz and S.H. Leventhal. Numerical solution of linear partial differential equations of elliptic-hyperbolic type**work partially supported by the office of naval research under contract nr044-453 and by the naval surface weapons center independent research fund. In BERT HUBBARD, editor, *Numerical Solution of Partial Differential Equations-III*, pages 55–88. Academic Press, 1976.
139. Pavol Sermer and Rudolf Mathon. Least-squares methods for mixed-type equations. *SIAM Journal on Numerical Analysis*, 18(4):705–723, 1981, <https://doi.org/10.1137/0718047>.
140. H. Bateman. SOME RECENT RESEARCHES ON THE MOTION OF FLUIDS. *Monthly Weather Review*, 43:163–170, 1925.
141. J.M. Burgers. A mathematical model illustrating the theory of turbulence. volume 1 of *Advances in Applied Mechanics*, pages 171–199. Elsevier, 1948.
142. G.B. Whitham. *Linear and Nonlinear Waves*. Pure and Applied Mathematics: A Wiley Series of Texts, Monographs and Tracts. Wiley, 2011.
143. Gary N. Felder, Lev Kofman, and Alexei Starobinsky. Caustics in tachyon matter and other Born-Infeld scalars. *JHEP*, 09:026, 2002, hep-th/0208019.
144. Miguel Alcubierre. The Appearance of coordinate shocks in hyperbolic formalisms of general relativity. *Phys. Rev. D*, 55:5981–5991, 1997, gr-qc/9609015.
145. Miguel Alcubierre and Joan Masso. Pathologies of hyperbolic gauges in general relativity and other field theories. *Phys. Rev. D*, 57:4511–4515, 1998, gr-qc/9709024.
146. Miguel Alcubierre. Hyperbolic slicings of space-time: Singularity avoidance and gauge shocks. *Class. Quant. Grav.*, 20:607–624, 2003, gr-qc/0210050.
147. Bernd Reimann, Miguel Alcubierre, Jose A. Gonzalez, and Dario Nunez. Constraint and gauge shocks in one-dimensional numerical relativity. *Phys. Rev. D*, 71:064021, 2005, gr-qc/0411094.
148. Randall J. Leveque. *Numerical Methods for Conservation Laws*. Lectures in mathematics ETH Zürich. Birkhäuser Basel, 2013.
149. C.M. Bender and S.A. Orszag. *Advanced Mathematical Methods for Scientists and Engineers I: Asymptotic Methods and Perturbation Theory*. Springer New York, 2013.
150. J.K. Kevorkian and J.D. Cole. *Multiple Scale and Singular Perturbation Methods*. Applied Mathematical Sciences. Springer New York, 2012.
151. Lin-Yuan Chen, Nigel Goldenfeld, and Y. Oono. The Renormalization group and

singular perturbations: Multiple scales, boundary layers and reductive perturbation theory. *Phys. Rev. E*, 54:376–394, 1996, hep-th/9506161.

152. Teiji Kunihiro. A Geometrical formulation of the renormalization group method for global analysis. *Prog. Theor. Phys.*, 94:503–514, 1995, hep-th/9505166. [Erratum: *Prog.Theor.Phys.* 95, 835 (1996)].

153. Yoshiki Kuramoto. On the Reduction of Evolution Equations in Extended Systems. *Progress of Theoretical Physics Supplement*, 99:244–262, 06 1989, <https://academic.oup.com/ptps/article-pdf/doi/10.1143/PTPS.99.244/5316511/99-244.pdf>.

154. Shin-Ichiro Ei, Kazuyuki Fujii, and Taeiji Kunihiro. Renormalization group method for reduction of evolution equations: Invariant manifolds and envelopes. *Annals Phys.*, 280:236–298, 2000, hep-th/9905088.

155. José T. Gálvez Ghersi and Leo C. Stein. Numerical renormalization-group-based approach to secular perturbation theory. *Phys. Rev. E*, 104(3):034219, 2021, 2106.08410.

156. Luc Blanchet. Gravitational Radiation from Post-Newtonian Sources and Inspiralling Compact Binaries. *Living Rev. Rel.*, 17:2, 2014, 1310.1528.

157. Manuel Tiglio and Aarón Villanueva. Reduced order and surrogate models for gravitational waves. *Living Rev. Rel.*, 25(1):2, 2022, 2101.11608.

158. Gregory B. Cook. Initial data for numerical relativity. *Living Rev. Rel.*, 3:5, 2000, gr-qc/0007085.

159. Gregory Walter Horndeski. Conservation of charge and the einstein–maxwell field equations. *Journal of Mathematical Physics*, 17(11):1980–1987, 1976, <https://doi.org/10.1063/1.522837>.

160. Iain Davies and Harvey S. Reall. Well-posed formulation of Einstein-Maxwell effective field theory. 12 2021, 2112.05603.

161. Jr. York, J. W. Kinematics and dynamics of general relativity. In L. L. Smarr, editor, *Sources of Gravitational Radiation*, pages 83–126, January 1979.

162. Marcus Ansorg, Bernd Bruegmann, and Wolfgang Tichy. A Single-domain spectral method for black hole puncture data. *Phys. Rev. D*, 70:064011, 2004, gr-qc/0404056.

163. Jeffrey M. Bowen and James W. York. Time-asymmetric initial data for black holes and black-hole collisions. *Phys. Rev. D*, 21:2047–2056, Apr 1980.

164. Steven Brandt and Bernd Bruegmann. A Simple construction of initial data for multiple black holes. *Phys. Rev. Lett.*, 78:3606–3609, 1997, gr-qc/9703066.

165. Félix-Louis Julié and Emanuele Berti. $d + 1$ formalism in Einstein-scalar-Gauss-Bonnet gravity. *Phys. Rev. D*, 101(12):124045, 2020, 2004.00003.

166. Carlos A. R. Herdeiro and Eugen Radu. Asymptotically flat black holes with scalar hair: a review. *Int. J. Mod. Phys. D*, 24(09):1542014, 2015, 1504.08209.

167. Mark A. Scheel, Stuart L. Shapiro, and Saul A. Teukolsky. Collapse to black holes in Brans-Dicke theory. 1. Horizon boundary conditions for dynamical space-times. *Phys. Rev. D*, 51:4208–4235, 1995, gr-qc/9411025.

168. Mark A. Scheel, Stuart L. Shapiro, and Saul A. Teukolsky. Collapse to black holes in Brans-Dicke theory. 2. Comparison with general relativity. *Phys. Rev. D*, 51:4236–4249, 1995, gr-qc/9411026.

169. Jerome Novak and Jose M. Ibáñez. Gravitational waves from the collapse and bounce of a stellar core in tensor scalar gravity. *Astrophys. J.*, 533:392–405, 2000, astro-ph/9911298.

170. Davide Gerosa, Ulrich Sperhake, and Christian D. Ott. Numerical simulations of stellar collapse in scalar-tensor theories of gravity. *Class. Quant. Grav.*, 33(13):135002, 2016, 1602.06952.

171. Ulrich Sperhake, Christopher J. Moore, Roxana Rosca, Michalis Agathos, Davide

Gerosa, and Christian D. Ott. Long-lived inverse chirp signals from core collapse in massive scalar-tensor gravity. *Phys. Rev. Lett.*, 119(20):201103, 2017, 1708.03651.

172. Patrick Chi-Kit Cheong and Tjonne Guang Feng Li. Numerical studies on core collapse supernova in self-interacting massive scalar-tensor gravity. *Phys. Rev. D*, 100(2):024027, 2019, 1812.04835.

173. Roxana Rosca-Mead, Christopher J. Moore, Michalis Agathos, and Ulrich Sperhake. Inverse-chirp signals and spontaneous scalarisation with self-interacting potentials in stellar collapse. *Class. Quant. Grav.*, 36(13):134003, 2019, 1903.09704.

174. Roxana Rosca-Mead, Ulrich Sperhake, Christopher J. Moore, Michalis Agathos, Davide Gerosa, and Christian D. Ott. Core collapse in massive scalar-tensor gravity. *Phys. Rev. D*, 102(4):044010, 2020, 2005.09728.

175. Chao-Qiang Geng, Hao-Jui Kuan, and Ling-Wei Luo. Inverse-chirp imprint of gravitational wave signals in scalar tensor theory. *Eur. Phys. J. C*, 80(8):780, 2020, 2005.11629.

176. Da Huang, Chao-Qiang Geng, and Hao-Jui Kuan. Scalar gravitational wave signals from core collapse in massive scalar-tensor gravity with triple-scalar interactions. *Class. Quant. Grav.*, 38(24):245006, 2021, 2106.13065.

177. Hao-Jui Kuan, Jasbir Singh, Daniela D. Doneva, Stoytcho S. Yazadjiev, and Kostas D. Kokkotas. Nonlinear evolution and nonuniqueness of scalarized neutron stars. *Phys. Rev. D*, 104(12):124013, 2021, 2105.08543.

178. Hao-Jui Kuan, Arthur G. Suvorov, Daniela D. Doneva, and Stoytcho S. Yazadjiev. Gravitational waves from accretion-induced descalarization in massive scalar-tensor theory. 3 2022, 2203.03672.

179. Raissa F. P. Mendes, Néstor Ortiz, and Nikolaos Stergioulas. Nonlinear dynamics of oscillating neutron stars in scalar-tensor gravity. *Phys. Rev. D*, 104(10):104036, 2021, 2107.07036.

180. Justin Khoury and Amanda Weltman. Chameleon fields: Awaiting surprises for tests of gravity in space. *Phys. Rev. Lett.*, 93:171104, 2004, astro-ph/0309300.

181. Justin Khoury and Amanda Weltman. Chameleon cosmology. *Phys. Rev. D*, 69:044026, 2004, astro-ph/0309411.

182. Alexandru Dima, Miguel Bezares, and Enrico Barausse. Dynamical chameleon neutron stars: Stability, radial oscillations, and scalar radiation in spherical symmetry. *Phys. Rev. D*, 104(8):084017, 2021, 2107.04359.

183. Paolo Creminelli, Matthew Lewandowski, Giovanni Tambalo, and Filippo Vernizzi. Gravitational Wave Decay into Dark Energy. *JCAP*, 12:025, 2018, 1809.03484.

184. Paolo Creminelli, Giovanni Tambalo, Filippo Vernizzi, and Vicharit Yingcharoenrat. Dark-Energy Instabilities induced by Gravitational Waves. *JCAP*, 05:002, 2020, 1910.14035.

185. E. Babichev, C. Deffayet, and R. Ziour. k-Mouflage gravity. *Int. J. Mod. Phys. D*, 18:2147–2154, 2009, 0905.2943.

186. Alexander A. H. Graham and Rahul Jha. Nonexistence of black holes with noncanonical scalar fields. *Phys. Rev. D*, 89(8):084056, 2014, 1401.8203. [Erratum: Phys. Rev. D 92, 069901 (2015)].

187. Tomas Andrade et al. GRChombo: An adaptable numerical relativity code for fundamental physics. *J. Open Source Softw.*, 6:3703, 2021, 2201.03458.

188. Hans Bantilan, Pau Figueras, Markus Kunesch, and Rodrigo Panosso Macedo. End point of nonaxisymmetric black hole instabilities in higher dimensions. *Phys. Rev. D*, 100(8):086014, 2019, 1906.10696.

189. Tomas Andrade, Pau Figueras, and Ulrich Sperhake. Evidence for violations of Weak Cosmic Censorship in black hole collisions in higher dimensions. *JHEP*, 03:111, 2022,

2011.03049.

190. Lam Hui and Alberto Nicolis. No-Hair Theorem for the Galileon. *Phys. Rev. Lett.*, 110:241104, 2013, 1202.1296.
191. Andrea Maselli, Hector O. Silva, Masato Minamitsuji, and Emanuele Berti. Slowly rotating black hole solutions in Horndeski gravity. *Phys. Rev. D*, 92(10):104049, 2015, 1508.03044.
192. Kent Yagi, Leo C. Stein, and Nicolas Yunes. Challenging the Presence of Scalar Charge and Dipolar Radiation in Binary Pulsars. *Phys. Rev. D*, 93(2):024010, 2016, 1510.02152.
193. Robert Benkel, Thomas P. Sotiriou, and Helvi Witek. Black hole hair formation in shift-symmetric generalised scalar-tensor gravity. *Class. Quant. Grav.*, 34(6):064001, 2017, 1610.09168.
194. Robert Benkel, Thomas P. Sotiriou, and Helvi Witek. Dynamical scalar hair formation around a Schwarzschild black hole. *Phys. Rev. D*, 94(12):121503(R), 2016, 1612.08184.
195. Andrew Sullivan, Nicolás Yunes, and Thomas P. Sotiriou. Numerical black hole solutions in modified gravity theories: Axial symmetry case. *Phys. Rev. D*, 103(12):124058, 2021, 2009.10614.
196. Hector O. Silva, Caio F. B. Macedo, Thomas P. Sotiriou, Leonardo Gualtieri, Jeremy Sakstein, and Emanuele Berti. Stability of scalarized black hole solutions in scalar-Gauss-Bonnet gravity. *Phys. Rev. D*, 99(6):064011, 2019, 1812.05590.
197. Alexandru Dima, Enrico Barausse, Nicola Franchini, and Thomas P. Sotiriou. Spin-induced black hole spontaneous scalarization. *Phys. Rev. Lett.*, 125(23):231101, 2020, 2006.03095.
198. Carlos A. R. Herdeiro, Eugen Radu, Hector O. Silva, Thomas P. Sotiriou, and Nicolás Yunes. Spin-induced scalarized black holes. *Phys. Rev. Lett.*, 126(1):011103, 2021, 2009.03904.
199. Emanuele Berti, Lucas G. Collodel, Burkhard Kleihaus, and Jutta Kunz. Spin-induced black-hole scalarization in Einstein-scalar-Gauss-Bonnet theory. *Phys. Rev. Lett.*, 126(1):011104, 2021, 2009.03905.
200. Hector O. Silva, Helvi Witek, Matthew Elley, and Nicolás Yunes. Dynamical Descalarization in Binary Black Hole Mergers. *Phys. Rev. Lett.*, 127(3):031101, 2021, 2012.10436.
201. Matthew Elley, Hector O. Silva, Helvi Witek, and Nicolás Yunes. Spin-induced dynamical scalarization, de-scalarization and stealthness in scalar-Gauss-Bonnet gravity during black hole coalescence. 5 2022, 2205.06240.
202. José M. Martín-García et al. xact. <http://www.xact.es>.
203. José M Martín-García. xperm: fast index canonicalization for tensor computer algebra. *Computer physics communications*, 179(8):597–603, 2008.
204. David Brizuela, Jose M. Martin-Garcia, and Guillermo A. Mena Marugan. xPert: Computer algebra for metric perturbation theory. *Gen. Rel. Grav.*, 41:2415–2431, 2009, 0807.0824.
205. Justin L. Ripley. Review-horndeski-nr. <https://github.com/JLRipley314/Review-Horndeski-NR>.
206. R. Courant and D. Hilbert. *Methods of Mathematical Physics*. Number v. 2 in Methods of Mathematical Physics. Interscience Publishers, 1962.
207. Heinz-Otto Kreiss and Jens Lorenz. *Initial-Boundary Value Problems and the Navier-Stokes Equations*. Society for Industrial and Applied Mathematics, 2004, <https://epubs.siam.org/doi/pdf/10.1137/1.9780898719130>.
208. Michael E. Taylor. *Pseudodifferential operators and linear PDE*. Birkhäuser Boston,

Boston, MA, 1991.

- 209. Cathleen Synge Morawetz. The mathematical approach to the sonic barrier. *Bulletin (New Series) of the American Mathematical Society*, 6(2):127 – 145, 1982.
- 210. Earll M. Murman and Julian D. Cole. Calculation of plane steady transonic flows. *AIAA Journal*, 9(1):114–121, 1971, <https://doi.org/10.2514/3.6131>.
- 211. C. Armendariz-Picon and Eugene A. Lim. Haloes of k-essence. *JCAP*, 08:007, 2005, [astro-ph/0505207](https://arxiv.org/abs/astro-ph/0505207).
- 212. V. A. Rubakov. The Null Energy Condition and its violation. *Phys. Usp.*, 57:128–142, 2014, 1401.4024.
- 213. Eric Gourgoulhon. 3+1 formalism and bases of numerical relativity. 3 2007, [gr-qc/0703035](https://arxiv.org/abs/gr-qc/0703035).
- 214. Steven Weinberg. Effective Field Theory for Inflation. *Phys. Rev. D*, 77:123541, 2008, 0804.4291.
- 215. Daniel Grumiller and Nicolas Yunes. How do Black Holes Spin in Chern-Simons Modified Gravity? *Phys. Rev. D*, 77:044015, 2008, 0711.1868.